

UNCLASSIFIED

AD **409 747**

DEFENSE DOCUMENTATION CENTER

FOR

SCIENTIFIC AND TECHNICAL INFORMATION

CAMERON STATION, ALEXANDRIA, VIRGINIA



UNCLASSIFIED

NOTICE: When government or other drawings, specifications or other data are used for any purpose other than in connection with a definitely related government procurement operation, the U. S. Government thereby incurs no responsibility, nor any obligation whatsoever; and the fact that the Government may have formulated, furnished, or in any way supplied the said drawings, specifications, or other data is not to be regarded by implication or otherwise as in any manner licensing the holder or any other person or corporation, or conveying any rights or permission to manufacture, use or sell any patented invention that may in any way be related thereto.

AEDC-TDR-63-118

63-4-

CATALOGED BY DDC 409747
AS AD NO.

409 747



THE SIMULATION OF HIGH ENERGY PENETRATING RADIATIONS

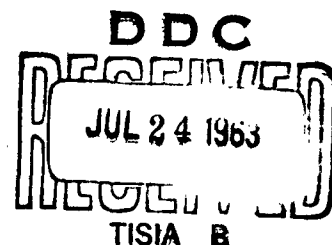
By

Sqd Ldr G. MacFarlane

RCAF

TECHNICAL DOCUMENTARY REPORT NO. AEDC-TDR-63-118

July 1963



(Prepared under Contract No. AF 40(600)-1000 by ARO, Inc.,
contract operator of AEDC, Arnold Air Force Station, Tenn.)

**ARNOLD ENGINEERING DEVELOPMENT CENTER
AIR FORCE SYSTEMS COMMAND
UNITED STATES AIR FORCE**

NOTICES

Qualified requesters may obtain copies of this report from ASTIA. Orders will be expedited if placed through the librarian or other staff member designated to request and receive documents from ASTIA.

When Government drawings, specifications or other data are used for any purpose other than in connection with a definitely related Government procurement operation, the United States Government thereby incurs no responsibility nor any obligation whatsoever; and the fact that the Government may have formulated, furnished, or in any way supplied the said drawings, specifications, or other data, is not to be regarded by implication or otherwise as in any manner licensing the holder or any other person or corporation, or conveying any rights or permission to manufacture, use, or sell any patented invention that may in any way be related thereto.

THE SIMULATION OF
HIGH ENERGY PENETRATING RADIATIONS

By
Sqd Ldr G. MacFarlane
RCAF

July 1963

ABSTRACT

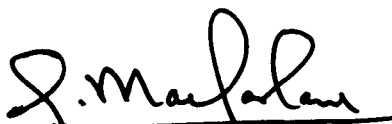
The basis of this study has been a search of current literature to determine the penetrating radiation characteristics of the space environments and to assess the necessity for reproducing such environments completely or in part.

This study of the radiation environments led to the formulation of some possible test objectives. The advantages and disadvantages of performing these objectives in the proposed chamber are listed.

Two main simulation approaches, one using radiation from isotopic sources and the other using particles generated by high energy accelerators, are feasible, but only the latter is worthy of consideration, taking into account the size of the vehicles to be tested. Furthermore, only the second method can provide a worthwhile match of the energy and flux spectra of space radiation.

PUBLICATION REVIEW

This report has been reviewed and publication is approved.



George MacFarlane
Sqd Ldr, RCAF
Engineering Division
Space Systems Office



Donald D. Carlson
Lt Col, USAF
Chief, Space Systems Office

CONTENTS

	<u>Page</u>
ABSTRACT	iii
1.0 INTRODUCTION	1
2.0 THE SIMULATION OF HIGH ENERGY PENETRATING RADIATION	
2.1 Discussion of the Penetrating Radiations	2
2.2 The Radiation Environments of Space	10
2.3 Penetrating Radiation Effects and Simulation Difficulties	26
2.4 Advantages and Disadvantages of Simulating Penetrating Radiations	33
3.0 CONCLUSIONS	
3.1 Summary of Environmental Data	36
3.2 Simulation Feasibility	37
3.3 Method A - Simulation using Isotopic Sources.	38
3.4 Method B - Simulation using High Energy Accelerators	38
4.0 RECOMMENDATIONS	39
REFERENCES.	57
APPENDIXES	
I. Typical Ranges of Energetic Particles	43
II. Radiation Dosages and Dose Rates.	45
III. Calculations	47
IV. High Energy Particle Accelerators	49

TABLES

1. Values of Relative Biological Effectiveness	5
2. Current Best Estimates of Van Allen Radiation Fluxes	13
3. I. G. Y. Flare Classification	24
4. Characteristics of Typical Accelerators	56

ILLUSTRATIONS

Figure

1. Mechanisms of Radiation Damage	9
2. Van Allen Belt Structure	12

<u>Figure</u>	<u>Page</u>
3a. Geomagnetic Field Influence on Cosmic Rays (Schematic)	17
3b. Forbush Decrease Mechanism (Schematic)	17
4. Structure of the Sun	19
5. Solar Plasma Cloud Influence	22
6. Magnetohydrodynamic Structure around the Earth	23
7. Cosmic Ray Dosage through Shielding	30
8. Dosages from Typical Solar Flares	34
9. Typical Alternating Gradient Accelerator.	53
10. Alternating Gradient Principle	54

1.0 INTRODUCTION

In the first five years of space flight, breakdown of communications and other electronic equipment due to degradation of solar cells and transistors caused by the various penetrating radiations in space have resulted in numerous, exasperating failures of unmanned earth satellites. With long-duration manned space flights in prospect, equipment reliability and crew confidence in the vehicle design would be greatly enhanced if it were possible to test* the complete vehicle and its operating sub-systems in the penetrating radiation environments of space. Such a simulation feature would make use of the built-in nuclear capability of a proposed space environmental facility.

Typical tests that might be run include:

- a. determination of damage to the exterior surface of a space vehicle caused by sputtering. Such damage might profoundly alter the emissivity, reflectivity, and absorptivity of temperature-controlling surfaces and so change critically the internal thermal environment of the vehicle. Collectors for solar power conversion devices to generate electrical power for use in flight or at a lunar base and astronomical telescope mirrors are also susceptible to sputtering damage. Such damage would reduce collection efficiency.
- b. investigation of the formation and reversion of color centers in exterior paint and optical glass
- c. determination of the performance of communications equipment, telemetry, navigational equipment, and flight control equipment containing semi-conductor devices such as solar cells, transistors, metallic rectifiers, etc.
- d. measurement of radiation dosages at crew positions, shelters, and other selected locations
- e. investigation of the effectiveness of various shielding configurations, equipment layout, and different combinations of shielding material

*This study was, in fact, suggested by several members of the Ad Hoc Committee on the Review of Design Criteria for an aerospace environmental chamber. The Committee met with members of the Space Systems Office at Arnold Air Force Station on August 28-29, 1962.

Manuscript received May 1963.

- f. study of the interaction of high vacuum, sharp temperature differentials, intense ultra-violet radiation, and high energy particle radiation on materials such as metals, hydrocarbons, plastics, polymers, and glasses and
- g. calibration and proper positioning of plasma and high energy particle measuring devices.

2.0 THE SIMULATION OF HIGH ENERGY PENETRATING RADIATION

2.1 DISCUSSION OF THE PENETRATING* RADIATIONS

2.1.1 The Types of Penetrating Radiations

The principal penetrating radiations comprise:

- a. protons,
- b. electrons,
- c. gamma and X-ray quanta

The first two are corpuscular (i. e. , possess a measurable rest mass), whereas the latter two are electromagnetic (i. e. , possess zero rest mass). The proton is the positively charged nucleus of the hydrogen atom. Hydrogen is by far the most abundant element in the universe and is the basic ingredient of the thermonuclear reaction that produces the stellar energy. The electron is a negatively charged particle with a mass $1/1836$ that of the proton. Gamma and X-rays are photon emissions. Gammas carry off surplus energy made available by re-arrangement in the energy state of nucleons within the nucleus, while X-rays perform the same function for energy released by electronic re-arrangements. The actual energy emitted (which determines the frequency and hence wavelength of the electromagnetic energy by Planck's Law, $E = h\nu$) depends upon the magnitude of the energy step undergone by the electron or nucleon. Thus X-rays can be of nuclear origin in some transformations. In actual

*The term "penetrating" is applied to those radiations whose energy is great enough to produce nuclear reactions or displacements at perhaps a considerable depth in a material. This is the chief distinguishing characteristic which separates the radiations considered in this paper from the electromagnetic radiation of the visible solar spectrum. Even ultra-violet radiation, the most energetic portion of the solar radiation, photoionizes atoms only a few atomic radii below the surface.

fact, the gamma and X-ray radiations are not distinct entities but merely possess different frequencies.

In addition to these four types, various other penetrating radiations are found in space. Very high energy particles, called cosmic rays, form a continuous radiation background throughout the galaxy. Although cosmic radiation is composed primarily of protons, photographic emulsions exposed in space and in the upper atmosphere have trapped such heavy ions as tin (atomic no. 50) and iron (atomic no. 26). These ions are stripped of all electrons and consequently are very damaging. The incoming cosmic ray protons and ions may also smash the nucleus of an atmospheric atom, releasing charged π mesons (the nuclear binding force), neutrons, and other debris as secondaries (Ref. 1). The neutron, in turn, decays simultaneously into a proton, neutron, and neutrino. The π meson may cause further nuclear disintegrations in its passage through matter. If no collision occurs, the π meson in turn decays into a charged μ meson. This meson then decays into a photon-electron cascade.

Finally, a secondary radiation of major importance in the shielding problem is the continuous X-ray spectrum, called Bremsstrahlung, produced when a charged particle is decelerated in the coulomb field of the nucleus. Bremsstrahlung, since it is electromagnetic, is far more penetrating than the original charged particle. Furthermore, it is emitted omni-directionally and is subsequently scattered in its passage through matter. Therefore, it may contribute significantly to the radiation dose in a vehicle, and unfortunately, high density shielding with its attendant weight penalty is required for its attenuation.

2.1.2 Radiation Units

The unit of radiation dosage employed depends on the type of radiation under study. In X-ray work, the important parameter is the exposed dose. The unit used to measure this is the roentgen, where one roentgen produces 2.08×10^9 ion pairs cm^{-3} . For gamma and neutron irradiation, a measure of the absorbed dose is required. For such measurements, the radiation unit (rad) is used. One rad equals 100 erg g^{-1} of material. When high energy particles are involved, the roentgen-equivalent-physical (rep) is sometimes used*. The energy equivalents of the roentgen and the rep are 83.7 erg g^{-1} and 93 erg g^{-1} , respectively. The last unit to be mentioned is the roentgen-equivalent-man (rem). The rem is a measure of the overall biological effect of penetrating radiations on humans or selected human organs or tissues.

*This unit is obsolescent and is being replaced by the radiation unit (rad).

For metals, ceramics, semi-conductors, etc., the radiation effects (Ref. 2) are proportional to the exposure dose, whereas the absorbed dose is a more useful parameter to evaluate radiation effects on organic and most inorganic compounds.

2.1.3 Radiation Terms

2.1.3.1 Range

The range of a nuclear particle is expressed in terms of g cm^{-2} . In the case of a charged particle, this range is the average depth of penetration corresponding to the given particle energy. For electromagnetic radiation, the range refers to the depth by which the intensity of the incident radiation has fallen by the fraction e^{-1} . The actual penetration depth in any given material is found by dividing the range by the density of the material under consideration. Typical ranges for various energies of the main types of particles are given in Appendix I.

2.1.3.2 Cross-Section

The probability that a nuclear reaction will occur is expressed in terms of a cross-section; the larger the cross-section the higher the probability that interaction will occur.

At low energies, the cross-section is high, and the classical type of collision (termed billiard ball collision) occurs between the incoming particle and the target atom. As the energy of the particle increases, the cross-section decreases. Now the usual mechanism of collision is the meshing of the electronic shells of the incoming particle and target atom. At still higher energies, the energetic particle does not remain for a sufficiently long period in the vicinity of a shell electron for interaction to occur. The only type of collision possible is that of an impact with the nucleus. Since the nucleus is very small compared to atomic dimensions, the cross-section is correspondingly very small.

Thus the intensity of displacement decreases with increasing proton energy. In the case where the incoming radiation is electronic, the intensity of displacement increases up to a certain electron energy from relativistic considerations; i. e., the electron increases in mass up to energies of a few Mev, with a resulting increase in its momentum. In ionization events, the same pattern is evident. The high energy particle leaves a long trail of ionization that increases in density (the effect known as "thin-down") as the particle energy decreases, but the effective radiation dose for a low energy particle is much higher than for a high energy particle since the former creates a dense pattern of ionization in a restricted volume.

2.1.3.3 Relative Biological Effectiveness

To correlate the biological effect of different types of radiation, the Relative Biological Effectiveness (RBE) was introduced. The RBE is also used to take account of the different sensitivities of different tissue and organs to the same type and energy of radiation. The RBE is expressed as the ratio of the dose of 250 Kev X-rays to the dose of the other radiation for the same biological effect. Typical values are tabulated below:

TABLE 1
VALUES OF RELATIVE BIOLOGICAL EFFECTIVENESS

Radiation (Ref. 3)	RBE	Radiation (Ref. 4)	RBE
fast neutrons	10	recoil nuclei	20
slow neutrons	5	alpha	10
protons	1-5-215	electron, 0.03 Mev	1.7
electrons, gamma, meson	1	gamma, X-ray, conversion electron	1

The concept of an RBE is complicated by the dependence on the conditions of exposure, the type of tissue, and the histological effect under consideration. For example, protons with energies less than 50 Mev have been assigned an RBE = 5 (Ref. 5), while for higher energies the value is RBE = 1. The variation is related directly to the different capture cross-sections of low and high energy protons.

2.1.4 Basic Mechanisms of Radiation Damage

Penetrating radiation causes damage by two main mechanisms: ionization (Ref. 6) and displacement (Refs. 7 and 8).

2.1.4.1 Ionization

In ionization, the incoming radiation transfers some or all of its energy and momentum to one or more of the shell electrons. The electrons are knocked out of their position in the shell, leaving the atom in a chemically reactive state. The excited atom may combine with neighboring atoms or molecules to form "odd" molecules. Almost all the energy of protons, electrons, and Bremsstrahlung ends up as ionization.

2.1.4.2 Displacement

Atomic displacement is the second damage mechanism. When high energy particles encounter matter, their velocity is so high that their

interaction time with the electrons in the shell is so very small as to be negligible. Energy loss occurs only when the particle collides with the nucleus of the target atom. The nucleus gains sufficient energy and momentum to escape from the crystal lattice position, dragging its electron covering with it.

If the energy of the original atom is very high, each target atom may liberate many other atoms before its energy is degraded sufficiently. These displaced atoms normally end up at odd points in the lattice structure. Such atoms are called interstitial. An increase of ten percent in the normal atomic density caused by interstitial atoms (Ref. 9) creates very large pressure pulses (in the order of 10^{11} dynes cm^{-2}). These pulses are converted to heat, producing a thermal spike (Refs. 10 and 11).

The heat pulse is of very short duration. The displaced atoms flow back randomly into the crystal structure. If the material has impurities (deliberate or accidental) in it, the spike promotes diffusion and disorder in the crystal, and the crystal properties are altered for better or worse. In some cases, the metallic atoms and/or the impurity atoms form minute pure crystals during the recovery phase. Such crystals may "grow" by attracting atoms of the element that lie outside the spike zone. The random rearrangement of atoms is called a displacement spike.

2.1.4.3 Sputtering

The sputtering process (Ref. 12), also called impact evaporation, is closely allied to the displacement problem. Two main theories have been advanced. The first is the "hot spot" Evaporation Theory. In it, the impacting particle transfers its energy to the local surface, heating a volume of atomic dimensions sufficiently high that the enclosed atoms evaporate. However, the results of recent experiments do not substantiate this theory (Ref. 13). The second is the Momentum Transfer Theory. In this theory, the incoming ion, or neutral particle, transfers sufficient momentum to a surface-bound atom to liberate the latter from the lattice.

There are several variations of the Momentum Transfer Theory, but no single one explains all the facts (Ref. 13). One discrepancy is in the basic value of the sputtering yield (the number of bound atoms freed per impact). This number varies greatly with energy. For example (Ref. 12), the sputtering efficiency for protons at 5 Kev is less than 0.1, while for an oxygen atom at the same energy it is 5.0. In general, the yield is a maximum in the energy range from 6 to 12 Kev. The yield is also a function of the angle of incidence, being a minimum for normal incidence, increasing to a maximum at about 70 deg and then decreasing for still smaller angles. The lattice parameters also affect the yield, as preferential sputtering is noticeable along cleavage planes and at grain boundaries. Further careful research is required in this area.

2.1.5 Specific Radiation Damage

2.1.5.1 Biological Damage

Radiation effects on humans can be classified into two main groups: genetic and somatic. In the former, the ionizing event causes a permanent lesion in a reproductive cell. This lesion is propagated as a malformation of one or more of the offspring. In the second group, the ionizing radiation acts to shorten the life* of the exposed individual, perhaps by initiation of a cancer or perhaps simply by accelerating the aging process.

The actual mechanism (Ref. 14) of cell damage is complicated. Genetic damage is caused by gene displacement or actual chromosome breakup. Most of the somatic damage is apparently the result of oxidation of the enzymes (which perform the energy interchange between the cell nucleus and the bloodstream) by the radiation. It is a general feature of radiation damage that a portion is reversible. This is accomplished either by unharmed cells taking over the function of dead cells or by simple recuperation of cells that are only slightly affected. Thus duration of exposure and intensity of the dose are important parameters.

It has also been found that a person's tolerance to radiation damage is strictly an individual reaction (Ref. 5) that cannot be forecast without actual exposure. Appendix II lists the maximum permissible dosages and typical dose rates encountered in space.

No data are available on radiation damage reversion under zero gravity considerations.

2.1.5.2 Degradation of Materials

Ionization events are unimportant in metals and similar conductors (Ref. 8) since displaced electrons merely diffuse into the electron gas and quickly fall back to their lower energy levels. The released energy appears as heat. In semi-conductors, ionization increases the number of carriers, but the effect is not permanent. Similarly, insulators exhibit higher values of conductivity, but the alteration is not permanent. New compounds may be formed in organic materials due to random recombination of the ionized atoms of the molecules. Polymer substances are most susceptible (Ref. 15) since the molecular chains are either permanently broken or cross-linked with neighboring broken chains to cause increased hardness and reduced elasticity.

*It has been estimated (Ref. 5) that a one-rem dose reduces life expectancy by fifteen days.

Displacement events alter permanently the properties of all substances except those where the atoms are free (as in a gas or a liquid) or where the temperature is sufficiently high and the crystal structure such that the displaced atoms can acquire sufficient thermal energy to return to open lattice positions. Thus, in general, bulk properties are altered. In ionic substances, the electrons displaced migrate through the crystal and create color centers at points of dense concentration. In semi-conductors, the displacement process produces (Ref. 16) defects which decrease the minority carrier lifetime. Silicon semi-conductors are affected critically by this process, while germanium (Ref. 2) is a hundred times more resistant.

Semi-conductor damage is critically dependent upon both energy and flux. Low energy protons have been found (Ref. 17) to cause greater permanent damage than the higher energy ones, a finding that is in line with cross-section considerations. Shielding of silicon solar cells with sapphire windows 0.25 g cm^{-2} thickness has resulted (Ref. 16) in no obvious damage as a result of electron or proton bombardment. However, a similar method of shielding was tried by Hulten, et al (Ref. 17) with negative results. The quartz shield stopped direct proton-produced damage, but the darkening of the quartz from color center formation decreased the amount of sunlight transmitted, thus reducing the power.

Displacements may also produce (Refs. 2 and 18):

1. a stabilization of phases in a temperature region outside the normal stability region of that particular phase
2. a meta-stable phase in a supersaturated alloy and
3. increased hysteresis losses and reduced permeability of magnetic alloys.

2.1.6 Summary

Generally speaking, biological damage, which is proportional to the linear energy transfer and hence to the number of ion pairs produced when a charged particle penetrates matter, is therefore primarily an ionization mechanism. The prime cause of damage to metals, semi-conductors, inorganic insulators, plastics, glasses, and ceramics can be attributed to displacement effects involving dislodgement of atoms from the crystal or molecular structure. Figure 1 attempts to summarize these effects in a broad manner. The basic radiations are located on the left of the page. The various processes by which the various types of radiation degrade and produce other types of radiation are indicated, and the feedback paths are shown. The diagram explains the intricacy of the radiation damage mechanism.

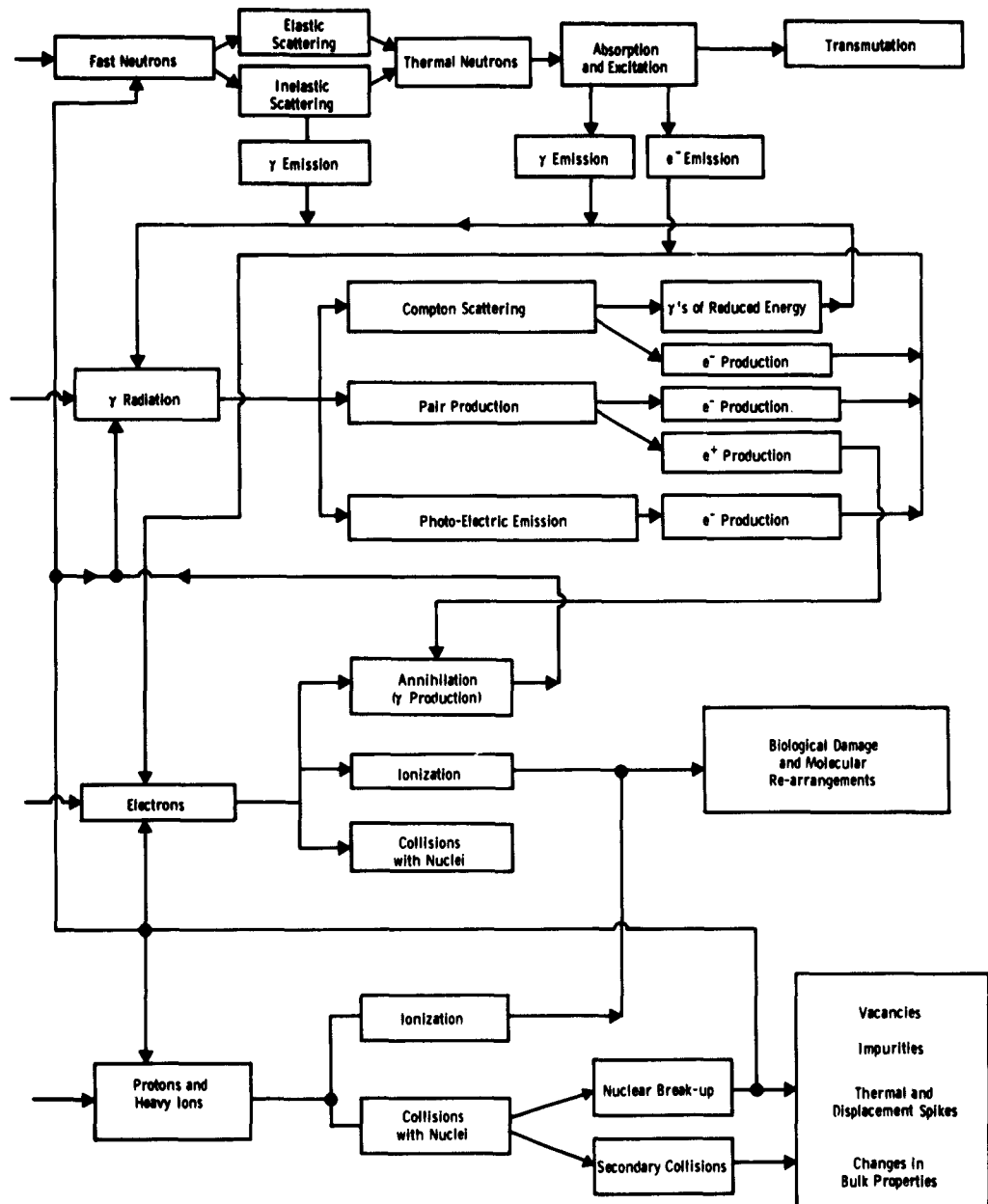


Fig. 1 Mechanisms of Radiation Damage

2.2 THE RADIATION ENVIRONMENTS OF SPACE

2.2.1 Introduction

The principal penetrating radiation environments that a satellite or a space vehicle encounters are:

- a. the ionosphere
- b. the auroral zone
- c. the Van Allen radiation belts
- d. galactic and extra-galactic cosmic rays
- e. the solar plasma and
- f. solar cosmic rays.

The physical characteristics of these environments, insofar as these are known, will be discussed. The type of radiation damage that might be expected and the necessity and practicality of duplicating each environment will be discussed in section 2.3.

2.2.2 The Ionosphere

The ionosphere consists (Refs. 19 and 20) of a succession of four distinct ionized layers that blend into one another. The lowest level is the "D" layer, lying between 60 and 85 km. This layer is believed to be formed by photo-dissociation of atmospheric atoms by solar Lyman α (1216\AA) radiation. It is thickest and most dense at local noon and disappears completely at night. Because the local air density is high, the electron collision frequency is high, and the region is therefore a strong absorber of electromagnetic energy.

The next highest layer is the "E" layer, lying between 85 and 140 km. Photo-ionization is believed to be initiated by solar X-ray radiation, and the densest electron concentration occurs at local noon. Occasionally, a very thin, intense layer, a few kilometers thick - called the sporadic "E" layer - forms within the main "E" layer, and the result is abnormal radio propagation.

The upper two layers are the "F"₁ and "F"₂ layers. Radiation emitted by the HeII ion at 304\AA is believed the cause. The layers are very distinct in the daytime but amalgamate during the night hours. Both regions possess the highest ion concentration in the ionosphere - about 2.5 to 4.0×10^5 electrons cm^{-3} - at local noon. The altitude of peak density is about 300 km. Above this, the electron concentration falls off

very slowly as the altitude increases. At 1000 km, the degree of ionization is unity (Ref. 19); i. e., the plasma and neutral concentrations are equal.

2.2.3 The Auroral Zones

Unlike the ionosphere which girdles the globe and stretches from pole to pole, the auroral zones (Ref. 21) are limited in extent, being confined to a crown-like region located about 65°-70° north and south geomagnetic latitude. They are regions of intermittent luminosity, which is produced by the collision of earth-aimed charged particles with atmospheric atoms. As a result of the collision, the electrons in the outer shells of the gas atoms have their energy levels raised. Subsequent electronic relaxation produces the visible glow. The characteristic colors produced are a function, of course, of the magnitude of the electronic excursion and the type of gas atom involved. These luminous displays generally occur between 100 to 120 km altitude, but occasional bursts have been measured at altitudes of 700 to 1200 km.

One reference (Ref. 22) advances strongly the Chapman-Ferraro theory to account for the formation of this activity. The basic tenet of this theory is that the charged particles involved are protons emitted by the sun. However, an alternate theory (Ref. 23), which fits in better with the latest satellite observations, has been put forward. In this theory, the charged particles are not of solar origin but are present all the time in the upper atmosphere. When an earth-bound solar plasma cloud collides with the geomagnetic field, hydromagnetic (HM) shock waves are generated (Ref. 24) which propagate down to the earth's surface. In their passage, such HM waves accelerate the charged particles from thermal velocities to some tens of thousands of electron volts. The protons, having relatively high inertia, will remain at relatively low energies, while the electrons gain significant amounts. This latter theory is also used to explain the enhancement of the outer Van Allen belt during periods of solar activity.

The electron fluxes are quite high (Ref. 25) (about 10^8 electron cm^{-2} sec and higher). The energy range is about 10 Kev to 100 Kev.

2.2.4 Van Allen Radiation Belts

Radiation detectors carried on Explorer 12 have indicated (Ref. 26) that the inner and outer belts overlap noticeably and that the outer belt occasionally possesses two zones of maximum intensity. However, since previous measurements are strongly indicative of different origins for the particles in each major zone, the concept of two distinct zones will be maintained. Figure 2 illustrates a typical cross-section of the radiation zones.

Note: Fluxes and corresponding energy ranges are tabulated in Table 2, Best Estimates of Van Allen Belt Fluxes.

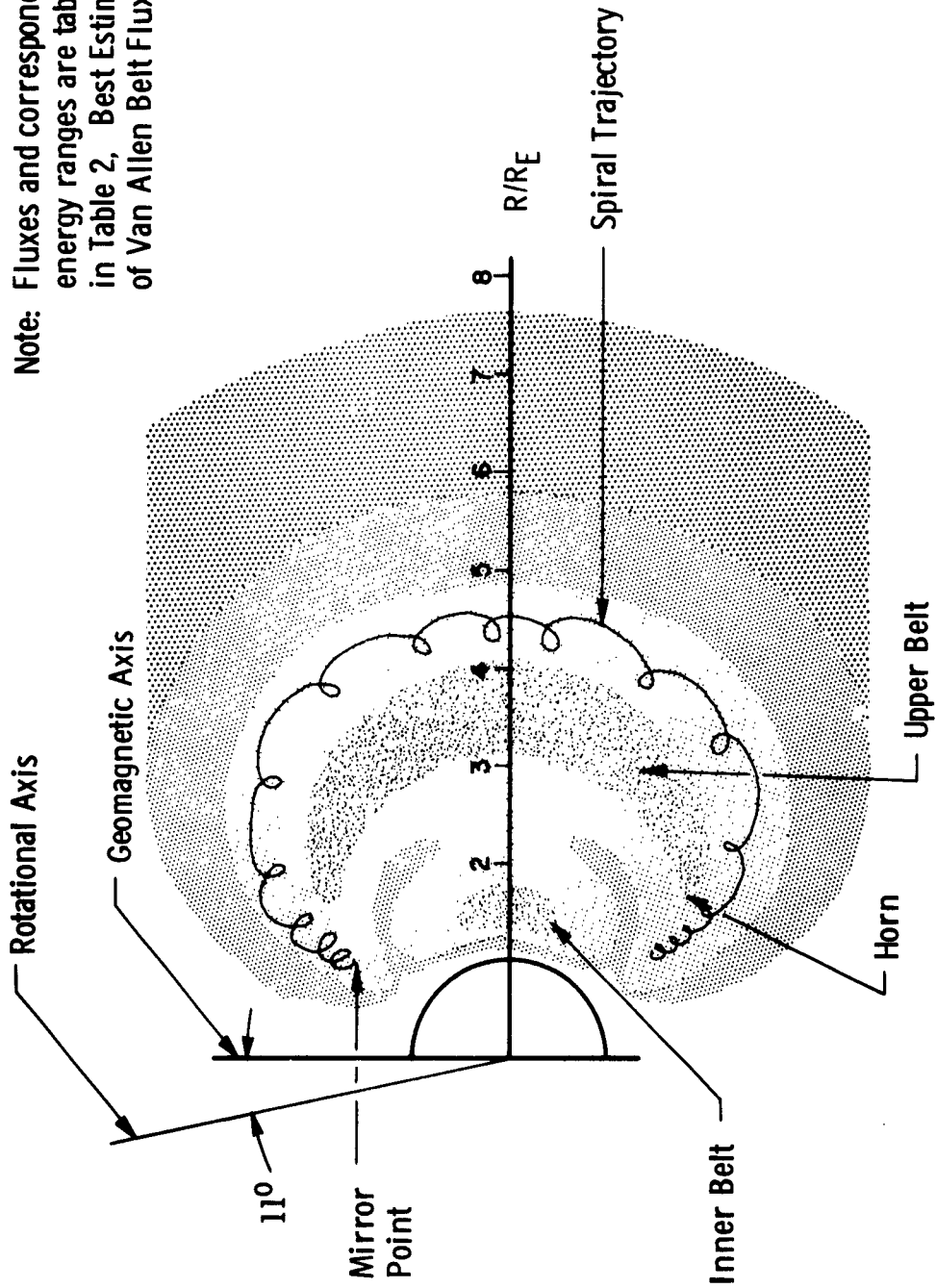


Fig. 2 Van Allen Belt Structure

TABLE 2
CURRENT BEST ESTIMATES OF THE VAN ALLEN RADIATION FLUXES

a. INNER ZONE PARTICLES

Particle	Energy Zone	Flux	Ref.
e ⁻	E > 20 Kev	$10^8 \text{ cm}^{-2} \text{ sec}^{-1} \text{ ster}^{-1}$	*
	E > 40 Kev	$10^7 \text{ cm}^{-2} \text{ sec}^{-1}$	*
	E > 2 Mev	$10^5 \text{ cm}^{-2} \text{ sec}^{-1}$	68
H ⁺	E > 100 Kev	$10^8 \text{ cm}^{-2} \text{ sec}^{-1} \text{ ster}^{-1}$	33
	E > 1 Mev	$3 \times 10^5 \text{ cm}^{-2} \text{ sec}^{-1} \text{ ster}^{-1}$	†
	E > 40 Mev	$2 \times 10^4 \text{ cm}^{-2} \text{ sec}^{-1}$	64

b. OUTER ZONE PARTICLES

Particle	Energy Zone	Flux	Ref.
e ⁻	E > 20 Kev	$2 \times 10^8 \text{ cm}^{-2} \text{ sec}^{-1} \text{ ster}^{-1}$	68
	E > 600 Kev	$5 \times 10^6 \text{ cm}^{-2} \text{ sec}^{-1} \text{ ster}^{-1}$	†
	1.6 Mev < E < 5 Mev	$2 \times 10^5 \text{ cm}^{-2} \text{ sec}^{-1}$	29
H ⁺	2 kev < E < 15 Kev	$5 \times 10^8 \text{ cm}^{-2} \text{ sec}^{-1}$	62
	E > 250 Kev	$10^6 \text{ cm}^{-2} \text{ sec}^{-1} \text{ ster}^{-1}$	††
	E > 60 Mev	$10^2 \text{ cm}^{-2} \text{ sec}^{-1}$	73

*L. A. Frank and J. A. Van Allen. "Intensity of Electrons in the Earth's Inner Radiation Zone." Journal of Geophysical Research. Vol. 68, No. 5, p. 1203. March 1, 1963.

†G. H. Ludwig. "Particles and Fields Research in Space." Proceedings of NASA - University Conference on the Science and Technology of Space Exploration, Vol. 1, p. 129. November 1 to 3, 1962.

††W. G. V. Rosser, et al. "Electrons in the Earth's Outer Radiation Zone." Journal of Geophysical Research, Vol. 67, No. 12, p. 4533. November 1962.

2.2.4.1 Inner Belt

In the lower altitude belt, it develops that the electron and proton fluxes are comparable. The latest estimates of the flux are given in Table 2.

The most notable feature of the inner belt is its stability. The intensity remains almost constant, even during periods of intense solar flare activity. Photographic emulsions flown through the belt have not yielded any detectable amounts of deuterium or tritium, the presence of which would be indicative of a solar origin.

The most probable source of the inner belt protons and electrons is the decay of albedo neutrons, (Ref. 26) produced by nuclear disintegration of atmospheric atoms by cosmic rays or high energy protons from the sun. Such neutrons decay into a proton, electron, and a neutrino. Comparisons (Ref. 27) of the theoretical energy spectrum and the measured energy spectrum are quite close and appear to validate the theory. However, not all authors (Ref. 28) agree with this.

The protons possess a long lifetime and decay principally by charge exchange with a neutral atmospheric hydrogen atom. The new charged proton is at thermal energy and effectively disappears from the view of any detector while the new neutral particle is no longer under the influence of the magnetic field, and it rapidly has its energy decreased to thermal level by collisions. Coulomb scattering of charged particles into the denser atmosphere is also an important loss mechanism, particularly for electrons in the vicinity of their mirror points. (The mirror point, the lowest altitude on the helical trajectory of a charged particle in the geomagnetic field, is the point at which the charged particle reverses direction for return to the other hemisphere.)

2.2.4.2 Outer Belt

The chief distinguishing features of the outer belt are as follows:

1. The trapped protons are much less energetic than the protons of the inner belt. In fact, early experiments seemed to indicate that protons were completely absent. However, detectors with low energy thresholds have measured appreciable low energy protons on recent flights.
2. When Explorer 12 data indicated that outer zone electrons were quite penetrating, the original estimate of the electron flux had to be reduced from 10^{11} electrons $\text{cm}^{-2} \text{sec}^{-1}$ to 10^8 electrons $\text{cm}^{-2} \text{sec}^{-1}$. The pioneering estimate had been based on a correction for the electron-to-Bremsstrahlung conversion efficiency. The latest flux estimates are given in Table 2.

3. The zone is extremely variable (Ref. 30) in both depth and intensity. Explorer 12 data indicate that the intensity varied by a factor of ten, up and down.
4. The penetrating particles present in the zone are thought to be telluric in origin, rather than of solar origin, for the following reasons (Refs. 31 and 32):
 - a. The solar plasma clouds have not been detected closer than a distance of eight to ten earth radii (Ref. 33). If such clouds did reach the outer belt zone, the contents of the region would escape rapidly into space due to the disruption of the geomagnetic field lines.
 - b. If the particles were injected from the solar plasma cloud, it would be expected that the intensity would increase during the active phase of a geomagnetic storm. However, the measured intensity drops (Ref. 30) during the active phase as a consequence of atmospheric heating increasing the air density and thereby causing increased scattering and absorption of the particles with low mirror points. During the main phase of the magnetic storm, the intensity should become steady or decrease if the solar plasma cloud were the source. Measurements indicate the opposite, since the particles gain energy during the random and violent geomagnetic field fluctuations (Ref. 34).

2.2.5 Galactic Cosmic Rays

2.2.5.1 Composition

Cosmic rays of galactic or extra-galactic origin are very high energy particles (Ref. 1) (from 0.5 Bev to 20 Bev normally, but occasionally reach as high as 10^{10} Bev). These particles, called primaries, are really atoms which have been stripped of all electronic charge. The composition of the particles has been determined (Ref. 4) approximately as:

- 79 percent hydrogen
- 20 percent helium
- .78 percent carbon, oxygen, and nitrogen
- .22 percent atomic number greater than 10.

2.2.5.2 Magnetic Field Influence

Since the particles are positively charged, the geomagnetic and interplanetary fields affect the trajectories considerably. For example,

the geomagnetic field prevents low energy particles from reaching the earth's surface except at regions near the geomagnetic poles. This is illustrated schematically in Fig. 3a. Particles with higher energies are deflected less and, for a particle to reach the earth's surface at the geomagnetic equator, it must possess an energy of at least 15 Bev. This distribution is called the latitude effect.

Also, since the geomagnetic field deflects charged particles towards the east, counters facing westward register more impacts than those facing eastward. This is termed the east-west effect.

A third effect, of secondary importance, is the longitude effect, so called because the dipole approximation to the magnetic field of the earth lies about 11.5° off the axis of rotation.

The interplanetary field (Refs. 35, 36) also affects the flux that arrives at the earth. During periods of peak solar activity - when the solar magnetic field extends deep into space - the flux is about $1 \text{ particle cm}^{-2} \text{ sec}^{-1}$ at energies greater than 1 Bev. When solar activity is at a minimum, the solar magnetic field influence is restricted to the region closer to the sun. The cosmic ray flux then rises to $3 \text{ particles cm}^{-2} \text{ sec}$ with energies in excess of 100 Mev.

In particular, the magnetic shielding offered by the plasma in a solar cloud eruption produces very sharp decreases (from 10 to 30 percent) in the cosmic ray flux commencing when the cloud envelopes the earth. Such sudden decreases are called Forbush decreases. Figure 3b shows the basic effect.

There is also evidence (Ref. 35) of a small increase in activity for a short period immediately prior to the Forbush decrease. This enhancement is ascribed to the reflection of the cosmic ray particles by the advancing plasma cloud shock front.

2.2.5.3 Primaries and Secondaries

The flux of primary radiation is insignificant compared to the flux of secondary radiation generated when the high energy incoming primary collides with an atmospheric atom, causing the latter's nucleus to disintegrate. A variety of mesons are produced, while the excited nuclear fragments decay to a stable state by "evaporating" neutrons and protons over a period of time. Gamma emission also occurs.

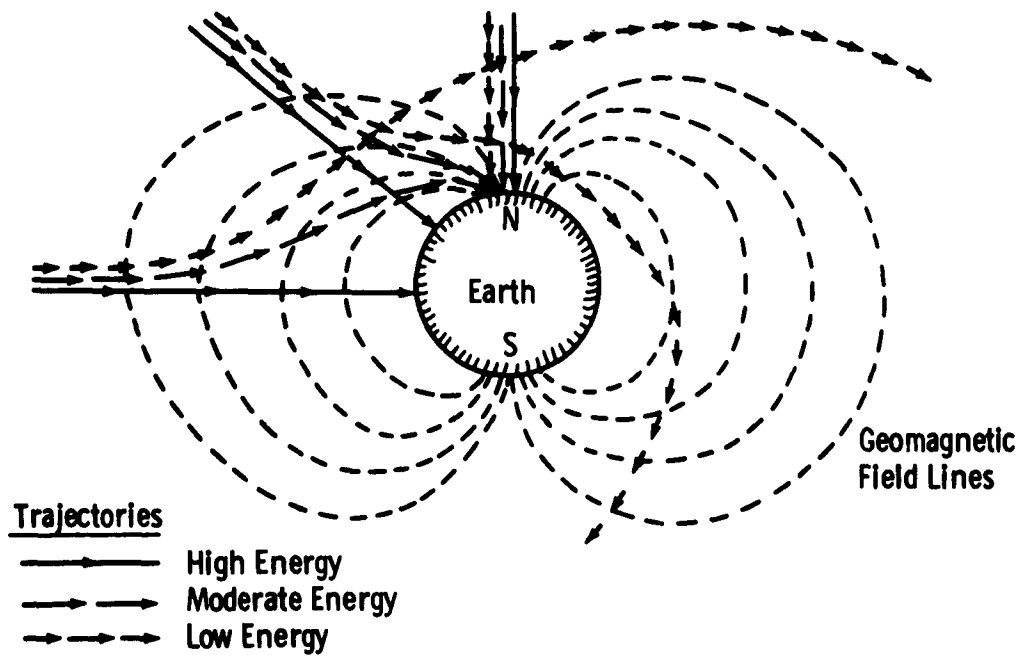


Fig. 3 (a) Geomagnetic Field Influence on Cosmic Rays (Schematic)

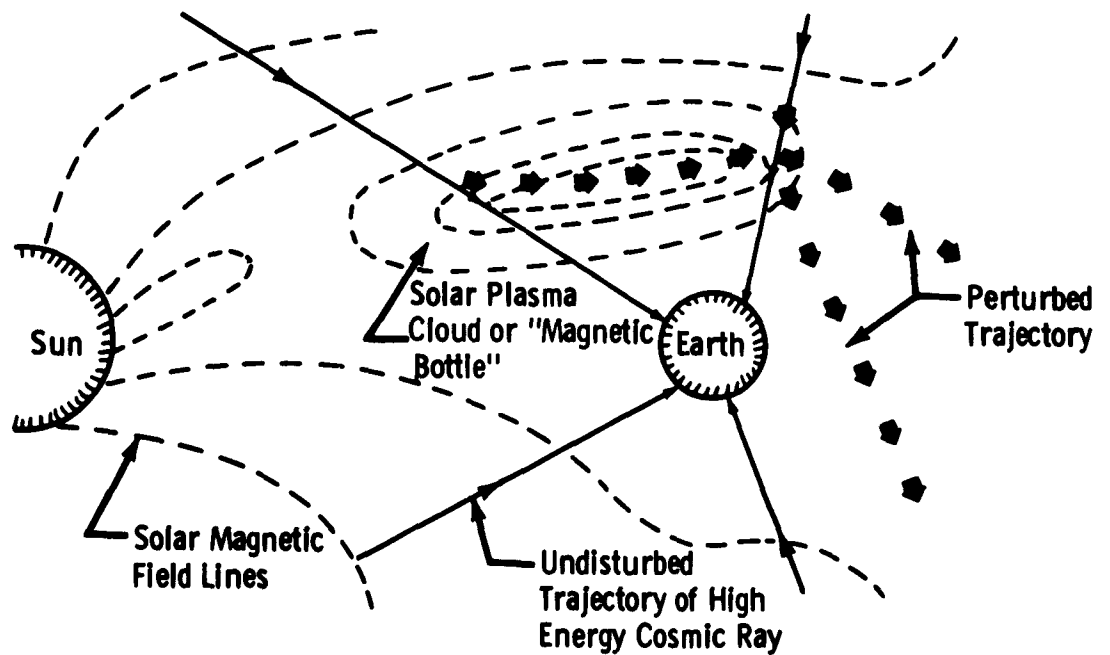


Fig. 3 (b) Forbush Decrease Mechanism (Schematic)

In the upper atmosphere, the most common meson emitted, a charged Π meson, decays into a μ meson if no other nucleus is encountered. The μ meson, in turn, decays into photons. In denser material, such as shielding, the Π meson may initiate a shower of nuclear collisions, each with meson production, that continues until the energy of the individual nucleons falls below the critical break-up threshold.

2.2.6 Solar Plasma

2.2.6.1 Solar Physics and Structure

The sun is classified by astronomers as a class G star, which implies that it is a member of one of the most abundant star groups. Its composition is 80 percent hydrogen, 19 percent helium, and traces of other elements. Since the sun is the focal point and the energy source of our planetary system, it is thought worthwhile to discuss its structure (see Fig. 4) and behavior in some detail. Following are the main zones (Ref. 37) of the sun:

1. core
2. convective zone
3. photosphere
4. chromosphere
5. corona

The core is the region of the sun in which the temperatures and pressures are so great that a stable, sustained thermonuclear reaction occurs. The resulting energy is then transferred to the surface through the convective zone principally by radiation, although near the surface, also by convection. The actual transfer mechanism has not yet been satisfactorily explained. The photosphere is the region which determines the radiative properties of the sun. It has a thickness of 0.001 radii, a density of about $10^{-8} \text{ g cm}^{-3}$, and a pressure of 5 torr (one torr = one mm Hg). These values are for the outer surface; inner surface values are multiplied by fifty. High altitude photographs have disclosed that the surface is quite granulated, the granules being irregular, polygonal-shaped bright patches, 300 to 1800 km in diameter, and with an appearance similar to that of convective cells. The chromosphere is the next layer, 10,000 km thick. It is marked by a series of abrupt temperature increases as different ions in succession reach their maximum radiative efficiency. The top of the chromosphere is irregular and transitory. Fine jets of matter, called spicules, protrude hair-like from the top, and their presence is indicative of instabilities in the solar plasma. Finally, there is the corona or solar atmosphere. It is highly tenuous, with a particle density of about $3 \times 10^7 \text{ cm}^{-3}$. The particles are highly ionized, with Fe_{10} , Fe_{14} , and Ca_{13} being observed. Surging out of the corona are the solar prominences. These have much higher particle densities, indicating that they must be supported by strong magnetic fields.

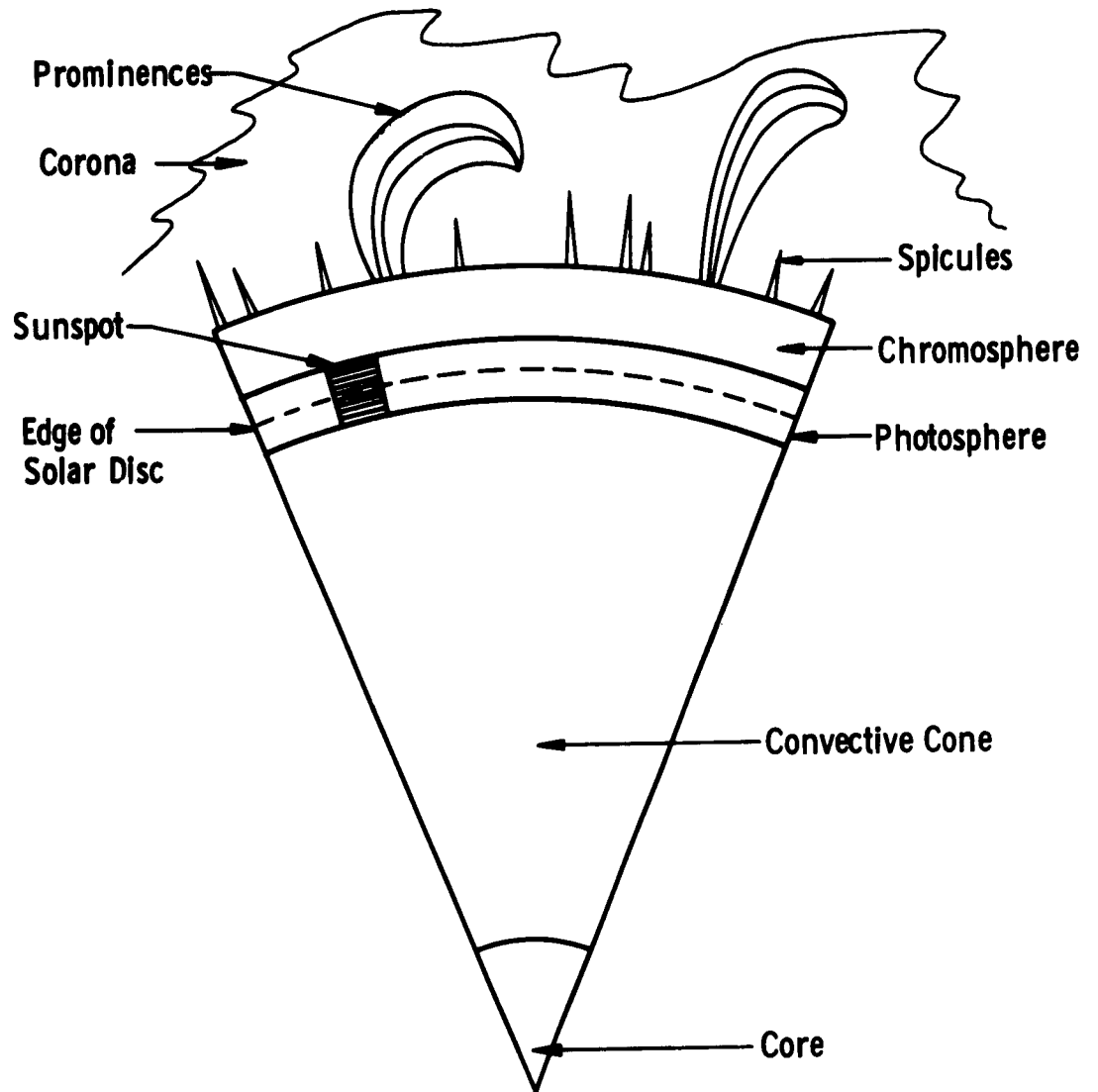


Fig. 4 Structure of the Sun

Two types of spots are regularly (Ref. 38) observed on the photosphere, one bright and one dark. The bright spot, called a facula, is a superheated cloud of gas. The dark spot is the familiar sunspot. Sunspots can occur singly but usually appear in clusters. They are cool regions at a temperature of 4500°K and are thus about 1500°K cooler than the surrounding photosphere. They are thought to be formed at points where convective clouds of ionized gases have dragged the solar magnetic field lines out into the chromosphere. The convective currents can rise up the field lines without difficulty but are inhibited by the field lines from moving sideways to close the loop. Thus the upper layers cool off, leaving the characteristic dark spot.

Observation of the sun in monochromatic light shows the surface to be covered with tuft-like clouds called flocculi. When these form aggregates around a sunspot, the result is termed a plage (or beach).

2.2.6.2 Solar Radio Noise

The motion of ionized gases through strong magnetic fields generates considerable electromagnetic noise in the radio frequency band. Astronomers classify this noise as follows: Type 1 noise occurs in bursts of extremely short duration. Type 2 and 3 noises are called slow and fast drift noise, respectively. The frequency of these noises decreases with time, indicating that the source is moving outwards through the corona. The source emits at the plasma frequency, which, of course, decreases as the electron density decreases. Type 4 emission is a long-lived noise. Its transmission is almost always a sign that corpuscular radiation is occurring. It is generated by the synchrotron emission (radiation generated by a particle undergoing circular motion in a changing magnetic field) of electrons trapped in a magnetic cloud that is close to the sun and free to move in the corona.

2.2.6.3 Plasma Characteristics

Solar plasma appears to originate in two different ways. First, there is evidence (Ref. 39) of a steady, slow diffusion of coronal gas outwards from the sun. This diffusion was termed the solar "wind" by early writers (Ref. 40), who obtained rough densities of 500 to 1000 particles cm^{-3} at a velocity of 1000 k sec^{-1} . The latest measurements, including those made by the Mariner II Venus probe (Refs. 41, 42), yield a density of about 20 particles cm^{-3} in a velocity range from 350 k sec^{-1} to 700 k sec^{-1} . The second plasma outlet is the disturbed region on the solar surface that often gives rise to a flare (Ref. 43). This plasma cloud is composed of electrons and protons at energies less than 100 Kev. The cloud density

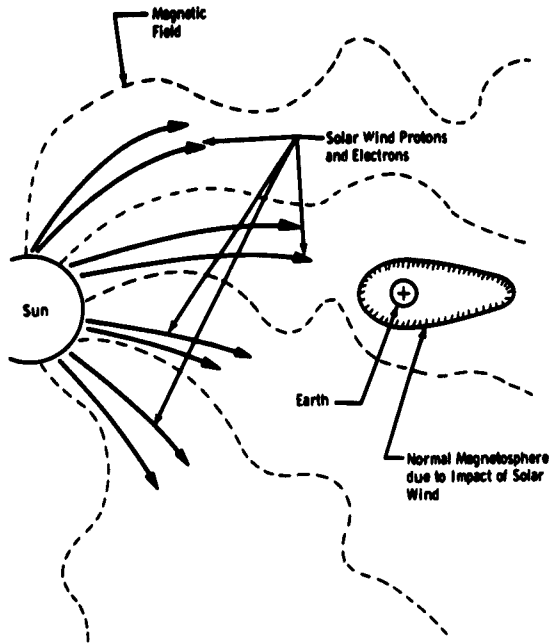
(Ref. 44) is perhaps 10^3 to 10^6 particles cm^{-3} , and its velocity is in the range of 1000 to 1500 km sec^{-1} . As the cloud leaves the solar surface, some loops of the solar magnetic field are dragged out into space by the plasma (see Fig. 5). There is good evidence (from radio emissions) that the clouds reach as far as the orbit of Jupiter.

As the solar plasma streams past the earth, it distorts (Ref. 45) the geomagnetic field from a symmetrical shape. The field facing the sun is compressed to about 65,000 km altitude as in Fig. 5d; on the night side, the field streams out in a tear drop configuration to perhaps 140,000 km. The cavity so formed is called the magnetosphere (see Fig. 6). It appears to play an important role in the transfer of energy from the sun to the atmosphere, thereby influencing the terrestrial weather.

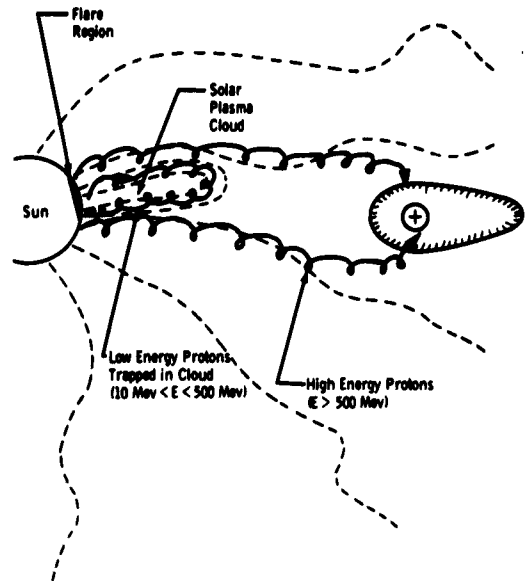
The impact of a plasma cloud on the geomagnetic field produces a Sudden Commencement (SC). This is the term given to the resulting violent fluctuations in the geomagnetic field strength. Simultaneously (Ref. 46) a Sudden Commencement Absorption (SCA) is detected by radio ionospheric opacity measuring devices (called riometers) that are tuned in to the galactic radio noise in the band between 27 mc and 50 mc. SCA has a short duration and is observed by stations near the maximum of the auroral zones on both the day and night sides of the earth. While the plasma cloud surrounds the earth, auroral noise absorption is detected. Unlike SCA, auroral absorption is highly irregular and lasts several hours. It is observed on both the day and the night sides. The cause is most probably due to Bremsstrahlung produced by electrons entering the upper atmosphere. Whether the electrons leak in through the interface of the plasma cloud and the geomagnetic field or are dumped from the outer Van Allen Belt during the magnetic field fluctuations, is a moot point and one which is not yet settled.

2.2.7 Solar Flare Proton Streams

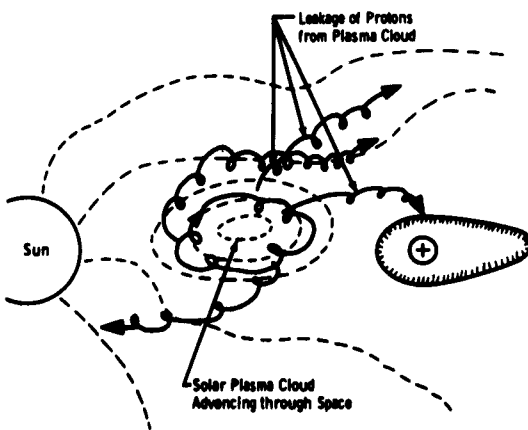
The solar flare is an explosive phenomenon (Ref. 47) occurring in the chromosphere. Other writers (Ref. 48) believe that the flare originates as a sub-photospheric disturbance in the internal solar plasma current. Flares are almost always associated (Ref. 49) with large complex groups of sunspots that possess large penumbral areas and well-developed plages (Ref. 50). It has been established that the most likely time for a flare is on the second passage of a well-developed plage group and associated penumbral area. The actual proton acceleration mechanism is undoubtedly some magnetohydrodynamic process, as protons with energies of 500 Mev are common and energies of 20 Bev are not unknown.



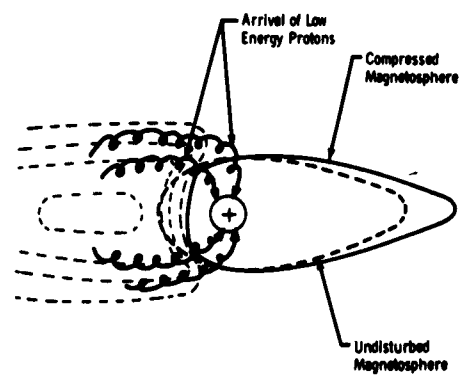
a. Normal Solar Interplanetary Magnetic Field Conditions



b. Formation of Plasma Cloud and Flight of Relativistic Protons



c. Plasma Cloud in Flight



d. Compression of Magnetosphere Due to Impact of Solar Plasma Cloud

Fig. 5 Solar Plasma Cloud Influence

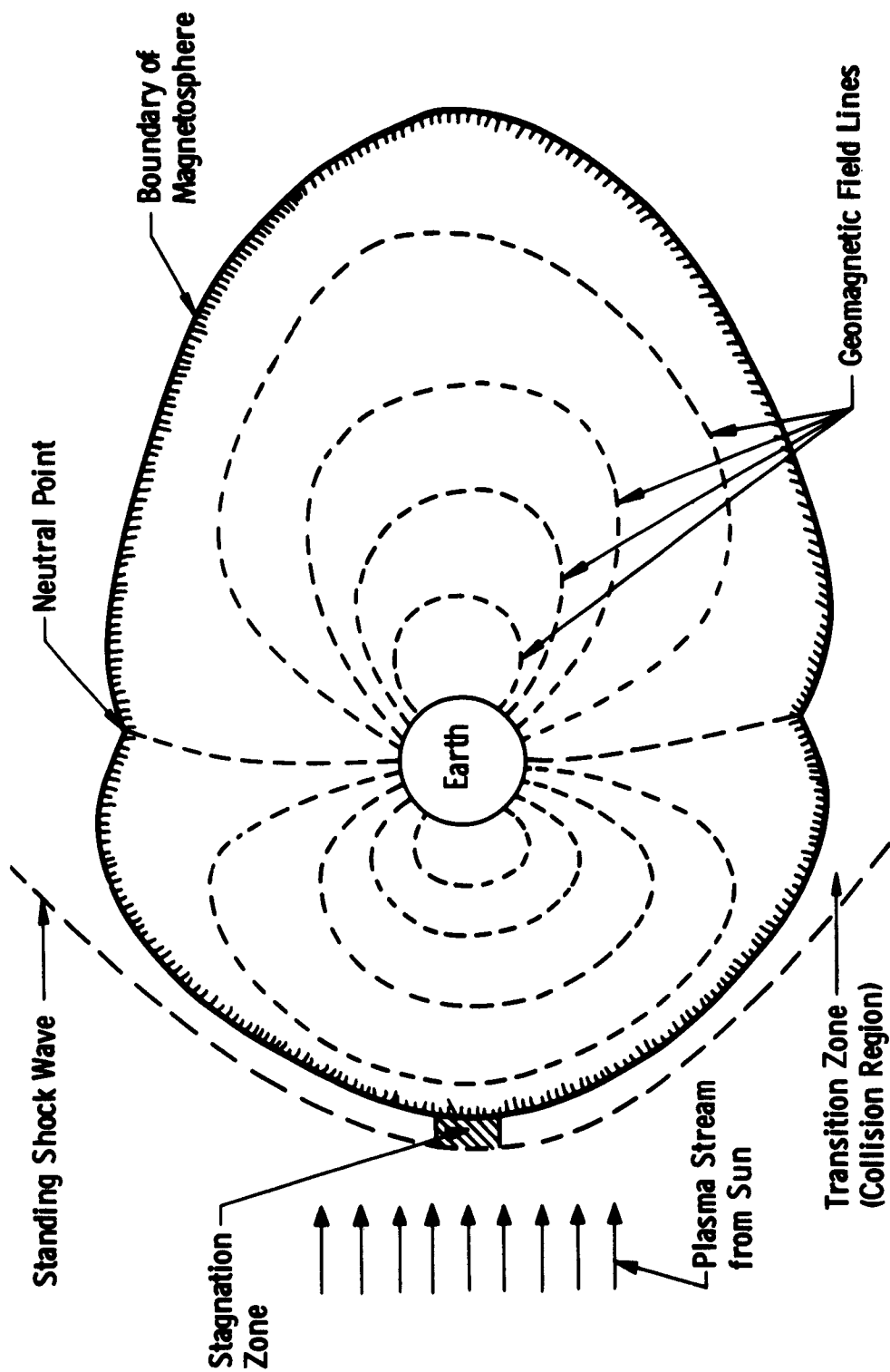


Fig. 6 Magnetohydrodynamic Structure around the Earth

Solar flare events can be conveniently classified (Refs. 29 and 51) into two main types: relativistic and non-relativistic. In relativistic events, the acceleration mechanism produces protons with energies in excess of 500 Mev. These events can be detected by direct measurement at the surface of the earth. Flares of this type are relatively rare, occurring about once every four years. In non-relativistic events, the proton energy ranges between 10 Mev and 500 Mev. Protons of these energies cannot be detected directly at the earth's surface. Instead, since the protons are charged, the geomagnetic field channels them into the polar regions (see Fig. 3a), producing the characteristic Polar Cap Absorption (PCA) (Ref. 52). PCA results from the additional ionization produced by the energetic protons in the "D" layer of the ionosphere (Ref. 43). This absorption is most intense on the sunlit side and usually lasts for the duration of the proton stream, about five to ten days. Although riometer measurements have been in existence only since the start of the International Geophysical Year (I. G. Y.), they already indicate that flares producing PCA occur monthly on the average. Refinements of instrumentation also permit some idea of the radiation dosages present in space to be obtained from the amount of absorption noted.

Sometimes, after a SC has occurred, these protons are detected at latitudes more southerly than those predicted by the particle energy. This is a result of the geomagnetic field disturbances associated with the arrival of the plasma cloud.

The flare itself has a duration ranging from a few minutes to a few hours, with the more intense flares generally having the longer duration. Generally, the proton flux, as observed at the earth, is constant for a period measured in a few hours. It then decays following a t^{-2} or t^{-3} law, although a noticeable flux may still be observed several days after an eruption. This indicates that the initial flux in such cases is very high and that some storage mechanism is operating in the space between the earth and the sun.

Flares are generally classified by the amount of area of the solar disc covered by them. The I. G. Y. classification and some typical statistics are set out in Table 3:

TABLE 3
I.G.Y. FLARE CLASSIFICATION

Flare Class	Percent Area of Solar Disc $\times 10^{-4}$	Percent in Class	Average Frequency of Occurrence	Duration of Emission
1	0-3	74	2 hr	17 min
2	3-7	22	daily	30 min
3	7-14	3	monthly	1 hr
3+	10	<1	4 yr	3 hr
4	>14	<<1	100 yr	n/a

During the I. G. Y., with a 95 percent coverage of the period from 1 July 1957 to 31 December 1958, 6,762 flares were observed (Ref. 53). The breakdown by class is as follows:

Class 3 or 3+	41
Class 2	497
Class 1	5,389
Class 1-	835

Many thousands of sub-flares are not included in this table.

A typical flare sequence and the events this sequence initiates might be as follows (Refs. 54, 55, and 56): The first sign is a bright spot on the solar disc. Simultaneously, Type 4 radio emission and strong X-ray and gamma bursts are observed. The latter electromagnetic radiation causes an increase in the ionospheric density. This increase is termed Sudden Cosmic Noise Absorption (SCNA)*. SCNA differs from PCA in that it is observed over the entire sunlit hemisphere and lasts only an hour or so. However, it plays havoc with short-wave communications during its lifetime.

If the flare is of the relativistic type, the proton stream reaches the earth in less than an hour. If it is non-relativistic, the time of flight is several hours (see Fig. 5b). The actual flight time is strongly dependent on the condition of the interplanetary magnetic field at the time of emission and thus depends upon previous solar activity. For example, the recent emission of a plasma cloud would have resulted in the establishment of magnetic lines of force directly connecting the sun and the earth, and the protons could be expected to utilize this channel for direct fast movement to earth as in Fig. 5b. On the other hand, if the interplanetary field is randomly arranged, the protons are scattered and must travel greater distances.

While the proton jet is being emitted from the sun, a plasma cloud of low energy protons and electrons is also being formed. The flight time of the plasma cloud is strongly dependent upon the interplanetary magnetic field conditions, as noted before.

If a second flare occurs while the first cloud is still between the sun and earth, three characteristic effects are observed. First, the high energy protons are scattered considerably and the PCA occurs slowly. This typifies the event as a "slow-riser." Secondly, the lower energy

*SCNA is sometimes referred to as a Sudden Ionospheric Disturbance (SID) (Refs. 20 and 37).

protons are trapped in the first cloud, and when this arrives at the earth, a very intense SCA occurs. Finally, as already noted, the second cloud travels faster and in a more direct manner than the first.

There are two other features of solar flares that must be mentioned. There is limited statistical evidence (Refs. 43 and 55) that protons produced by flares occurring on the western side of the disc travel more directly to earth than those emitted from the eastern side. The second feature pertains to the isotropy of direction of the protons. There is some reason to believe, mainly from certain directionality effects observed by instruments on the earth's surface (Refs. 43 and 47) that, at least during the initial phase, the proton stream is directional. However, late-arriving protons and especially those trapped in a plasma cloud that lies inside the earth's orbit are almost certainly isotropic as a result of the influence of stray and varying magnetic fields and scattering from collisions during the long flight time (see Fig. 5c).

2.3 PENETRATING RADIATION EFFECTS AND SIMULATION DIFFICULTIES

2.3.1 The Ionosphere

2.3.1.1 Typical Effects

One major effect on a satellite orbiting in this region is the build-up of a negative potential (Refs. 19 and 57) on the surface. The charge accumulation is the result of the satellite orbital velocity and the electron thermal velocity being larger than the positive ion velocity. The effect is reinforced by photo-electric emission caused by solar ultra-violet and X-ray radiation. Since plasma conditions prevail, the satellite is surrounded by a corresponding cloud of positive ions, whose density is several times greater than normal in front of the body (thereby increasing the induced charge density on this area) and perhaps 0.05 to 0.1 percent of normal behind the body. The linear dimension of the disturbed region behind the body is roughly equal to the mean free path. This cloud of charge has the following results:

1. A magnetohydrodynamic (MHD) drag is set up that extracts appreciable (Ref. 58) potential energy from the orbit.
2. The positive ion cloud increases considerably the radar cross-section (Ref. 59) of the satellite, rendering it more difficult to "blacken."
3. The ionized wake possesses good electromagnetic radiating and reflecting properties (Ref. 60).

4. The potential built-up on the vehicle and the presence of the cloud may seriously affect the operation of electrical propulsion units.
5. Measurement of the physical properties of the undisturbed plasma (such as composition, density, and velocity) by means of Langmuir probes is very difficult (Ref. 19), and careful data reduction is necessary to obtain the true values.
6. During vehicle ascent through the ionosphere, the ionic constituents may increase (Ref. 61) the rate of surface oxidation and corrosion.

A second major effect of the ionosphere is the refraction of electromagnetic waves in their passage through the layers. Below certain critical frequencies (which are functions of the ion density and hence correlated to a degree with solar activity), the waves are returned to earth or space, as the case may be. This effect causes small pointing errors (which might be serious in an anti-satellite defense system) in tracking systems.

Finally, noise in the form of amplitude and phase modulation is added to electromagnetic signals. This noise is generated by the fluctuating electron density. This noise source should be insignificant in comparison with the other types and powers of noise present.

2.3.1.2 Simulation Necessity

Simulation of all these ionospheric effects is not considered practical for the following reasons:

1. The greater (and more useful) part of the satellite's life is spent at altitudes in excess of 300 km.
2. Electromagnetic wave refraction and noise generation by the plasma are physical effects that require great distances in which to be demonstrable.
3. The ion cloud cannot be generated since it is a dynamic effect.
4. The wake cannot be generated since it also requires movement.

2.3.2 The Auroral Zones

Before simulation can be attempted, the energy spectrum and the types of particles responsible for the luminous displays must be known with greater certainty.

2.3.2.1 Typical Effects

The effects on the space vehicle can be considered confined to the surface layer because the energy of the electrons and protons is quite low. Also, electron-produced Bremsstrahlung is quite small at the energies under consideration.

A maximum electron flux of 10^{11} electrons $\text{cm}^{-2} \text{sec}^{-1}$ produces a surface dose of about 10^8 r hr^{-1} (Ref. 21). Such dosages produce temporary electrical transients in exposed insulators, and there may be cumulative long-term damage to thermal control and optical surfaces.

Since only a small fraction of the orbit time is spent within the auroral zone and since satellite altitudes lie above the zone of peak auroral activity (100 km), the radiation effects are not so severe as they appear at first glance. Calculations of the energy flux involved (see Appendix III, 1.0) show that the aurora contributes approximately $8 \times 10^{-4} \text{ watt cm}^{-2}$ at the peak flux of $10^{11} \text{ cm}^{-2} \text{sec}^{-1}$. This is insignificant when compared with the solar constant of $1400 \times 10^{-4} \text{ watt cm}^{-2}$.

2.3.2.2 Simulation Necessity

Simulation is not recommended since the required engineering design data can be obtained more cheaply at a particle accelerator facility, such as the Argonne National Laboratory. In any event, before simulation can be undertaken, the energy spectrum and the types of particles responsible for the luminous displays must be known with greater certainty.

2.3.3 Van Allen Belts

2.3.3.1 Inner Van Allen Belt - Typical Effects

The proton component is quite energetic and a dose rate of 120 r hr^{-1} has been estimated (Ref. 12) through 2 g cm^{-2} of shielding. This would be equivalent to an aluminum wall 0.3 in. thick. Shielding of this thickness would stop all protons possessing a high RBE. Additional shielding would be necessary, however, if long-term exposure were contemplated, but it would not be needed for short duration transit flights. The protons also adversely affect (Ref. 17) solar cells, although it is hoped that protective external coatings will help. For example, in one test (Ref. 62), cells protected by a 0.003-in. thick glass film showed a six percent power drop after exposure for 113 days, while unprotected cells lost 50 percent power during the first few orbits. However, the formation of color centers and darkening of the film can cut down transmittivity and nullify the protection afforded the actual semi-conductor material.

The electron component in the inner belt produces high surface doses and, since the energy is moderately high, Bremsstrahlung makes a contribution to the internal dose.

Sputtering is considered by most writers (Refs. 13 and 61) to be insignificant.

2.3.3.2 Outer Van Allen Belt - Typical Effects

The proton component (if it exists at all) is of very low energy, and only surface effects are likely. The electron component is also of low energy, although the very intense flux of $10^8 \text{ cm}^{-2} \text{ sec}^{-1}$ is a source of anxiety as this flux corresponds (Ref. 4) to a surface dosage of 10^4 r hr^{-1} .

One effect of high radiation doses on electronic equipment has already been noted, and one failure has been described in detail (Ref. 63). In this case, sudden decreases in signal strength were noted from a satellite when the latter was in the vicinity of the lower horn of the outer belt. The decrease was occasionally sufficient to reduce the signal power below the prevailing noise level. The cause was later traced to irradiation effects on the quartz crystal controlling the local oscillator. The resulting detuning of the transmitter caused the ground receiving station to lose the signal.

2.3.3.3 Simulation Necessity

Simulation should be attempted as satellites may be expected to make extended passes through the zones (and at least the lower fringes) if the orbit is sufficiently high and/or eccentric. Although manned operation in the Van Allen belts is unlikely, due to the requirement for heavy shielding for the crew and the guidance and flight control systems plus the lack of sufficient booster lifting capability, the use of electrical propulsion systems to drive large refueling and cargo satellites either into very high orbits or directly to the moon must be provisioned for in any new space simulation chamber design. It is conceivable that some cargoes will require radiation protection during the extended transit time through the two zones.

2.3.4 Cosmic Rays

2.3.4.1 Typical Effects

Instruments on Pioneer V have measured a cosmic ray flux of $2.5 \text{ particles cm}^{-2} \text{ sec}^{-1}$ in interplanetary space. This measurement has been translated into a dosage ranging from 0.45 rem wk^{-1} (Ref. 64) (with no

shielding but allowing for the extra contribution of the heavy primaries) to a dosage of 0.65 rem wk^{-1} (Ref. 5) (again based on no shielding but using an RBE of 5 to account for the contribution of heavy primaries). As the shielding thickness increases, the dosage increases due to secondary collisions and cascades, reaching a maximum value of 0.75 rem wk^{-1} and then decreasing (see Fig. 7). The reduction is due to the decreasing weight assigned to the RBE values for heavy primaries as the shielding thickness increases. It is significant, however, that approximately 25 g cm^{-2} of shielding is required to reduce the dosage inside the cabin to that of free space, and approximately 90 g cm^{-2} is needed to reduce the dose to the maximum allowable value of 0.3 rem wk^{-1} established by the Atomic Energy Commission. This level can be exceeded for short periods without harm, but it is restrictive when flights of several months' duration are undertaken.

Because of the low flux and great penetrating power of the primary particles, the reaction cross-section is small, and little damage to materials is expected. The main hazard is biological, but as previously mentioned, prohibitively large thicknesses are required to provide adequate shielding.

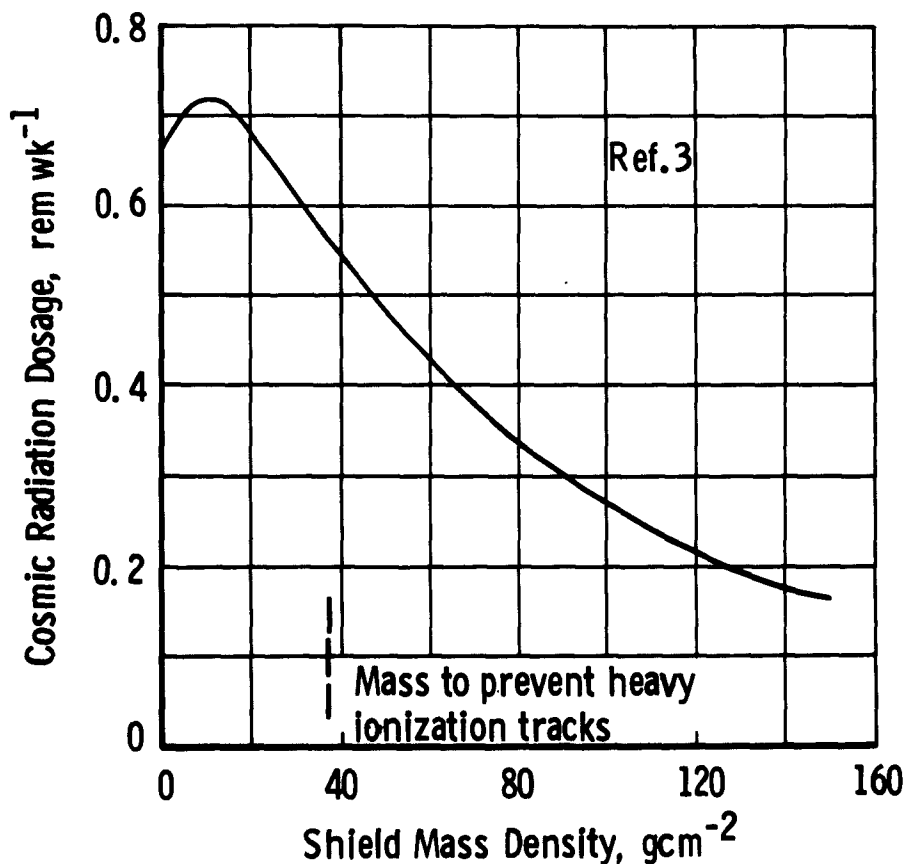


Fig. 7 Cosmic Ray Dosage through Shielding

2.3.4.2 Simulation Necessity

Simulation of the low energy protons and ions is possible, since the average velocity is 4 Bev, but simulation of the highest energy particles is almost impossible. The high energy obtained in an alternating gradient accelerator at Brookhaven National Laboratory is 32 Bev. However, some simulation, at least of the lower energies, should be attempted because it is recognized that the cosmic ray contribution alone approximates the maximum allowable weekly or yearly dosage in space.

Simulation is difficult. In space, the cosmic rays are incident on the vehicle from all directions. In a low earth orbit, the radiation is restricted to the upper surface of the vehicle, and the energy spectrum of the flux, in addition, varies with geomagnetic latitude.

2.3.5 Solar Plasma

2.3.5.1 Typical Effects

Since the electrons and protons comprising the solar "wind" and the solar plasma clouds are relatively low energy, the internal dosage is negligible, but the surface dose could be appreciable, perhaps as much as 10^6 rad hr⁻¹ (Ref. 21). Calculations of the energy flux of typical solar "wind" and plasma cloud conditions (see Appendix III, 2.0 and 3.0) show that the values of 5.6×10^{-7} watt cm⁻² and 1.2×10^{-4} watt cm⁻², respectively, are insignificant in comparison to the solar constant of 1400×10^{-4} watt cm⁻².

The principal effects likely on a satellite are:

1. damage to transistors and solar cells, principally by the protons
2. hydrogen embrittlement of metals exposed to a proton flux for long periods (The proton gains an electron by a charge exchange process inside the crystalline structure, and it stays within the lattice.)
3. degradation of plastics and elastomers
4. biological damage to personnel exposed without shielding in space and on the lunar surface
5. formation of color centers in optical glass and pigment-covered surfaces and
6. some sputtering of exposed surfaces about 30 \AA yr^{-1} (Ref. 13).

Opinions on this subject are varied. Some authors (Ref. 61) do not consider it serious; others do. For example, assuming a population ratio of the plasma as H:He Heavy ions to 75:6:0.06, an effective

sputtering ratio of 0.2 was developed (Refs. 65 and 66) for use with proton density figures. Assuming 600 particles cm^{-3} and a velocity of 1000 km sec^{-1} , an opaque 300 Å film would be removed in seven months.

2.3.5.2 Simulation Necessity

Simulation is certainly desirable on those vehicles likely to travel in interplanetary space. Generation of the plasma is difficult particularly with regard to the matching of the energy spectrum and flux requirements. Uniformity over the entire vehicle surface is also required. An additional aspect of such tests is that prolonged exposure time is needed.

2.3.6 Solar Protons

2.3.6.1 Typical Effects

The proton stream originating from solar flares is the most significant radiation parameter for biological damage and internal radiation levels in the vehicle. This flux must be considered in the design of manned and unmanned space vehicles, lunar base buildings, facilities, transportation, and general scope of operations on the moon and interplanetary space.

No accurate values of the solar flare flux is available, partly from ignorance and partly because each flare is individualistic in character. Estimates of the integral flux range from 30 protons $\text{cm}^{-2} \text{sec}^{-1}$ (Ref. 5) to 50-875 protons $\text{cm}^{-2} \text{sec}^{-1}$ (Ref. 67) to 10^4 protons $\text{cm}^{-2} \text{sec}^{-1}$ (Refs. 7 and 21) to 1.5×10^7 protons $\text{cm}^{-2} \text{sec}^{-1}$ (Ref. 68). In general, the integral flux can be approximated by the power law

$$N(\text{with energies} > E) = CE^{-5}$$

where

N = integral flux

E = energy

C = constant

This indicates that the flux of particles decreases rapidly as the energy increases. Calculations (see Appendix III, 4.0) show that the energy flux due to solar flare protons amounts to 3.2×10^{-8} watt cm^{-2} , which is insignificant when compared to the 1400×10^{-4} watt cm^{-2} of the solar constant.

Typical effects of solar flare protons are:

1. sputtering (Again, estimates are highly variable. One reference (Ref. 21) estimates the rate to be 36 \AA per 100 hr, while another estimates (Ref. 13) the loss at 3 \AA per flare.)
2. biological damage from both the primary and the secondary radiation (Dosages arising from typical flares are shown in Fig. 8.)
3. material damage, especially degradation of solar cells.

2.3.6.2 Simulation Necessity

The table on proton ranges (Appendix I, 1.0) illustrates that, using the commonly mentioned shielding thickness of 8 g cm^{-2} , a proton with energy in excess of 100 Mev would penetrate the shield. Since the human body absorbs protons of less than 350 Mev, protons of at least 450 Mev must be produced to simulate the proper biological dosage. Since, at energies in excess of 150 Mev, the incoming protons possess the capability of initiating meson production in matter, energies of this order would produce the desired secondary radiation as well. If 100 g cm^{-2} of shielding is arbitrarily chosen as the maximum feasible shield thickness, protons of 1 Bev are required.

Simulation of these protons is within the capability of presently operating accelerators. Calculations (see Appendix III, 5.0) using the data from Table 4 show that a flux of about $10^5 \text{ cm}^{-2} \text{ sec}^{-1}$ is easily achieved. However, at least two accelerators are required to irradiate the top and bottom of the vehicle simultaneously. It is also not possible to use only one type of accelerator to provide the energy range coverage in a series of successive steps due to the limitations of the accelerating process. A summary of the principle types of accelerators is presented in Appendix IV together with some construction features and design problem areas.

2.4 ADVANTAGES AND DISADVANTAGES OF SIMULATING PENETRATING RADIATIONS

From the material presented so far, the advantages and disadvantages of adding penetrating radiation simulation to an aerospace simulation chamber become clear. The advantages are:

1. If the proposed chamber is already designed with a nuclear capability, no additional shielding is therefore required for the chamber itself.

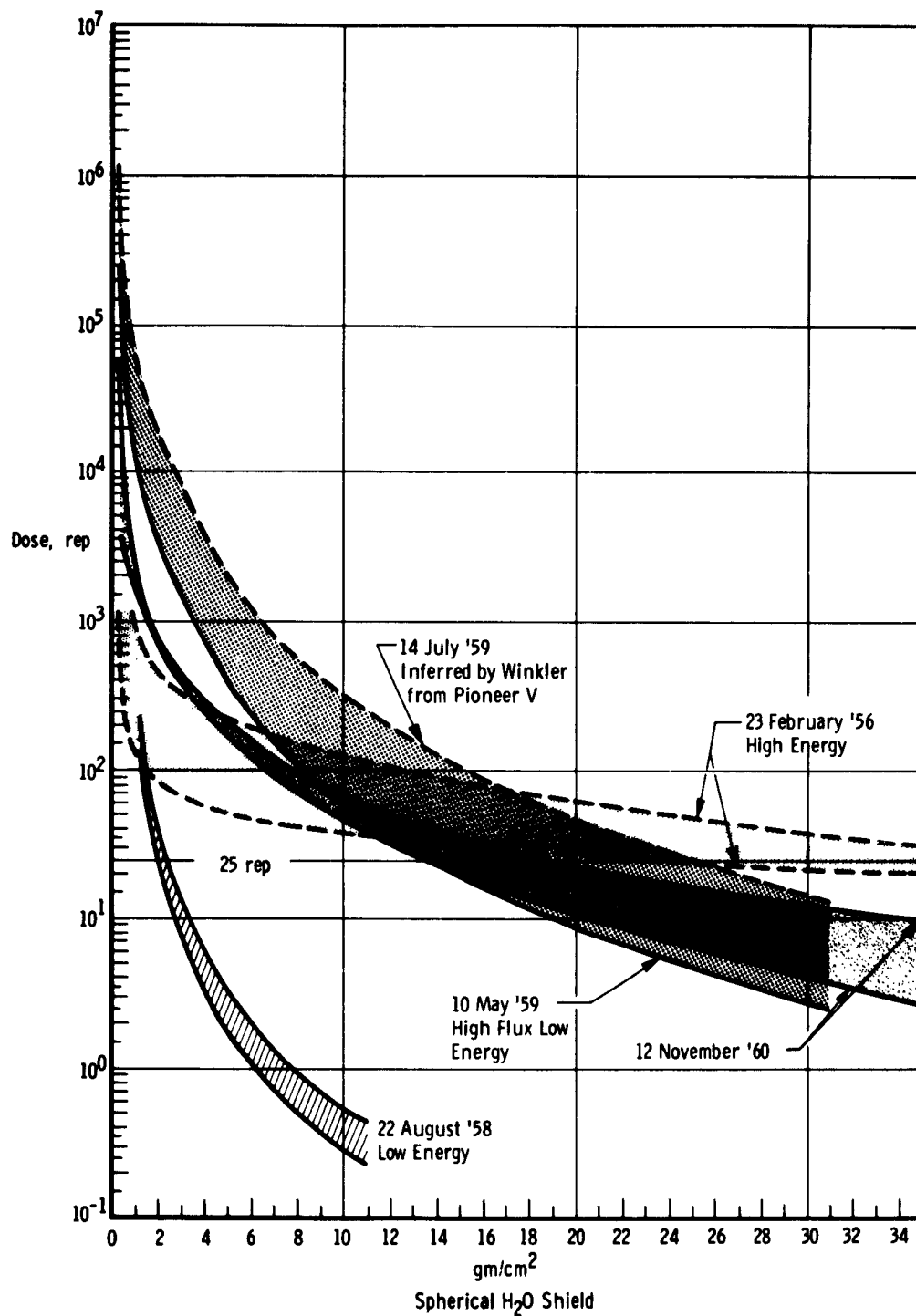


Fig. 8 Dosages from Typical Solar Flares (Ref. 4)

2. Accurate radiation dosages can be obtained for various crew positions using suitably instrumented anthropometric dummies. Such instrumentation would aid in the design of partial body shielding and movable shielding designs. For example, protection of the spleen would raise the threshold level for incipient radiation damage by a factor of two (Ref. 13).
3. Study of the effects of radiation on coated and painted surfaces and external equipment and sensors can be accomplished.
4. Lubricating problems of external and internal moving equipment (such as telescoping antennas, solar cell arrays, and floated gyroscopes) can be studied.
5. Ion engine operation and behavior of electronic equipment could be checked in a plasma environment.
6. Since the moon lacks both a shielding atmosphere (the earth's atmosphere is equivalent to 12 feet of aluminum (Ref. 6) or 1040 g cm^{-2} shielding thickness (Ref. 1)) and a significant magnetic field, operations on a lunar base are critically affected by solar plasma clouds and solar flare protons. Therefore, lunar equipment design and particularly protective clothing design, portable and mobile "fall-out" shelters for exploration use, assembly procedures, and construction techniques, require evaluation in a radiation environment.
7. Before the use of algae in a closed cycle ecological system can be considered, the photosynthesis process should be tested in a combination solar radiation - penetrating radiation environment. It is possible that, since the algae must be exposed to sunlight through minimum shielding for maximum process efficiency, the radiation dose may disturb the reproductive rate of the algae sufficiently to cause a fatal breakdown in the waste-to-oxygen cycle.
8. Fifteen to twenty years from now, active shielding using high intensity magnetic fields generated in superconducting coils (Refs. 69 and 70) is likely to have been developed to the point of practicality. The physical size of the proposed chamber would permit testing of at least scale models of such shield designs, using the available simulated space radiations.

The disadvantages are:

1. Several additional openings are required in the inner and outer shell of the chamber, thus reducing the cold wall area.
2. Electromagnetic and/or electrostatic deflecting equipment may have to be installed within the double-walled shell of the chamber,

introducing additional loads and requiring space. This equipment is required to provide a uniform coverage of all the surfaces of the vehicle because all the penetrating radiation environments are essentially isotropic in direction.

3. For true simulation, the energy spectrum and particle composition of the environment must be matched. This is most difficult since particle accelerators, by their basic design, produce one type of particle at one particular energy.
4. The energy spectrum and composition of the various environments are known only approximately at present. However, the accurate simulation required for, say, integrated total dosage behind shielding, requires correct basic data with which to start.
5. The fluxes of earth-tied radiation as well as those of solar plasma and protons and cosmic rays are latitude and time-dependent. At first glance, assumption of "worst case" conditions seems an excellent simplification. However, this approach overlooks the pressing need to shave useless weight in order to maximize mission payload and performance.

3.0 CONCLUSIONS

3.1 SUMMARY OF ENVIRONMENTAL DATA

A summary of the penetrating radiation fluxes and energies is as follows:

1. The auroral and ionospheric contributions mainly occur below typical satellite altitudes. Of the major phenomena, charge accumulation, enlarged radar cross-section, ionized wake, and refraction of electromagnetic waves, only the first can be simulated. The others are dynamic effects that require large distances to be noticeable.
2. Simulation of Van Allen radiation is a less complex problem. However, extended operation by manned vehicles in this region is unlikely for many years to come. This is the general consensus in the literature in this regard.
3. Solar proton streams from flares cause primarily a secondary radiation environment within the vehicle. This problem is one of design and a separate facility for such tests may be more economical in the long run.

4. The surface effects of solar plasma and flare protons in the chamber will be different from those encountered in actual space flight because the chamber density is orders of magnitude higher than the true space density and several orders of magnitude higher than the flare and plasma particle density. For example, the true space density is less than 3 molecules cm^{-3} , while the chamber density at 10^{-8} torr is 3×10^8 molecules cm^{-3} . The proton density in a plasma cloud (see Appendix III) may be 2×10^4 protons cm^{-3} . Thus the "surface cleansing" effects of solar plasma and protons will be greatly reduced.
5. Simulation of solar plasma and proton radiation at a lunar base requires that the radiation be incident vertically. This requirement is difficult to satisfy since the massive solar simulator is located in this position.
6. The critical component in the space flight system, as far as radiation is concerned, is the man. Individual reaction to radiation is a personal characteristic and tolerance can only be determined after exposure. By then, the man's usefulness in the program has ended. Thus testing of the reaction of flight crews to the internal radiation environment in the vehicle is not a valid objective. What is required is an evaluation of the shielding effectiveness at the crew positions and the design of shielding to pass the smallest possible dosage. It should be remembered that the doses from all radiation sources are additive and, although each source may be well below the danger level (see Appendix II), the cumulative dose may exceed the dangerous level, and one or more crew members may be so sufficiently incapacitated as to be unable to perform their assigned functions and duties.

3.2 SIMULATION FEASIBILITY

There are two approaches possible to the simulation of the penetrating radiation environment. Which one is chosen depends on the answers to the following questions:

1. What effects must be simulated:
 - a. If material and surface damage only are the important criteria, total dosage only is the important parameter, and Method A (to be described below) offers significant cost advantages.
 - b. If biological damage and shielding effectiveness only are important, Method B (to be described) must be employed.
 - c. If both the requirements of a and b must be satisfied, Method B must be employed.

2. How large is the vehicle surface to be exposed to the penetrating radiation?

If the vehicle is quite large (as are the vehicles the proposed chamber is designed to handle), Method B is much more attractive.

3.3 METHOD A - SIMULATION USING ISOTOPIC SOURCES

In this method, radioactive sources, comprised of various elements selected for their intensity, type of radiation, and energy spectrum, would be hung from a framework surrounding the test objective at distances calculated to ensure uniformity of flux and the proper flux intensity. This method is to be employed (Ref. 71) in a chamber at the Bell Aero Systems Co., Buffalo, New York.

The system is relatively cheap, as sources can be easily manufactured (and renewed if necessary) in existing nuclear reactors. They are shipped in lead containers, and routine handling precautions permit easy handling and removal when the simulation is not required. No elaborate storage is required.

There are several inherent difficulties. High energy particles are not available, and internal vehicle radiation is simulated with gamma radiation, whose passage through shielding is not comparable to proton passage. Lower energy gamma sources simulate the electron Bremsstrahlung. For coverage of large areas, the number of sources required and the structure required to support them, are likely to produce shadows that may interfere with proper solar simulation.

This method is best suited for tests involving time-integrated dosages on small specimens; i. e., material damage. However, tests involving materials only are more a design problem than a systems test objective and should not receive undue weight.

3.4 METHOD B - SIMULATION USING HIGH ENERGY ACCELERATORS

In this method, high energy particle accelerators of various types (see Appendix IV) are used to generate the type of particle in the proper energy range desired, and very accurate simulation is obtainable. By proper choice of energy range and type and number of accelerators, all radiation environments, with the exception of the very high energy cosmic rays (whose flux is very small anyway) can be produced.

The major drawback is the capital cost of the equipment, buildings, and shielding required. Several electron generators (probably of the

(Van de Graaff type or linear accelerator type) and a minimum of three proton accelerators (a cyclotron or linear accelerator covering the Kev and low Mev range, one synchrotron covering the 100 to 500 Mev, and a third covering the 500 Mev to 2 Bev range) are probably needed.

All accelerators require carefully built foundations, thick shielding walls, massive electromagnets, cooling facilities for the magnets, a vacuum system capable of evacuating the particle track to 10^{-6} torr, and a power source capable of handling large amounts of pulsed power. Initial alignment of the magnets and the beam focusing coils and electrodes is a skilled, time-consuming task. For example, thirty-one physicists, technicians, and engineers have spent almost one year aligning a 110-ft long linear accelerator (Ref. 72) that will be used to inject high energy protons into the main track of the 12.5 Bev zero gradient proton synchrotron at the Argonne National Laboratory. Thus it is obvious that Method B is expensive to build and that highly skilled operators are required to run and maintain the equipment. However, as far as test flexibility and facility growth potential are concerned, Method B is the only method worthy of consideration.

To spread the capital cost involved and to increase utilization of this expensive equipment, serious consideration should be given to locating additional facilities around the accelerator buildings, in which component, material, sub-systems, and scale-model tests could be conducted without interference to the primary systems testing in progress in the space environmental chamber.

4.0 RECOMMENDATIONS

1. Before a firm decision to implement Method B by installing high energy accelerators is made, it is suggested that a series of research programs be initiated to provide answers to the following questions:

a. What are the effects of particle radiation on material in a vacuum?

There is a considerable body of literature dealing with the effects of radiation on many different materials during their exposure to the atmosphere or their immersion in gases and solutions of various kinds. One such effect, for example, is greatly accelerated corrosion. However, little, if any, work has been done on damage in vacuum conditions, where corrosion effects are unlikely.

In addition, much of the damage information has been obtained from samples exposed to very intense neutron beams generated in nuclear

reactors. Since the proton-electron damage mechanism is not identical to the neutron damage mechanism, extrapolation of the results of neutron exposure to cover ionization type damage is unlikely to be valid.

b. How important an effect is sputtering?

As indicated in the body of the report, estimates of damage and importance vary widely. Laboratory experiments show that sputtering yield is dependent upon the purity of the ion beam, the type of ion used, and upon the hardness of the vacuum established. Since the ions used in the laboratory are quite "heavy" in order to provide measurable yields, the sputtering yield in such experiments is overstated in comparison to the yield of a pure proton beam. Therefore, an experimental program should be set up to establish the importance of sputtering, using a proton beam in a space vacuum environment.

c. What types of accelerators are required, and how many?

To answer this question, a detailed analysis of the energy spectra and fluxes of the environments to be simulated is required. Energy bands would be allotted to the different types of accelerators in such a fashion as to minimize costs while maintaining some flexibility in operation. This project would also determine whether real time simulation is feasible, again with cost as the criterion. A practical high energy cut-off point would also be chosen.

d. What problem areas exist when the accelerator complex is added to the proposed facility design?

Once the types and operating energy levels of the accelerators have been fixed, a siting plan, compatible with the existing design concept, if possible, should be developed. The shielding, electrical power, cooling, vacuum, and control system requirements should also be developed. Methods of extracting, diverging, and focusing the low and high energy particles should be examined and a solution obtained to the problem of "illuminating" all the exposed surfaces of the vehicle simultaneously and uniformly. Clashes with the existing design should be isolated so that corrective action can be taken.

2. Consideration should also be given to establishing a nuclear research facility for handling long-duration life tests of components and subsystems. This facility would permit full-time utilization of the accelerator complex. It would remedy to a considerable extent the present difficulty in obtaining accelerator time to conduct engineering experiments, as opposed to pure science research.

This facility would be useful in conducting scale-model tests in shielding optimization studies where the use of models would permit rapid changes

of materials and material thicknesses. Such tests should be carried out to verify the results of digital computer studies. The theoretical background is available to convert the model results to dosages in full-scale vehicles.

By introducing appropriate neutron targets into the proton beams from accelerators, strong neutron beams can be obtained. These beams could be used in conjunction with the proton and electron beams to evaluate the combined reactor-space radiation environment for sub-system tests without the need for activating a space power reactor.

APPENDIX I
TYPICAL RANGES OF ENERGETIC PARTICLES

1.0 PROTONS

<u>Energy, Mev</u>	<u>Range in H₂O, g cm⁻²</u>	<u>Range in Al, g cm⁻²</u>
1	.002	.003
10	.1	.14
50	2.0	2.7
100	8.0	11.0
200	30.0	41.0
500	100	137
1,000	300	410

2.0 ELECTRONS

<u>Energy, Mev</u>	<u>Range in Al, g cm⁻²</u>
1	.4
3	1.4
5	2.7

3.0 ALPHA PARTICLES

<u>Energy, Mev</u>	<u>Range in Al, g cm⁻²</u>
1	.005
5	.008
10	.016
20	.05
100	.96

4.0 γ RADIATION-MASS ABSORPTION COEFFICIENT

Energy, Mev	Al, cm ² g ⁻¹	H ₂ O, cm ² g ⁻¹	Pb, cm ² g ⁻¹
.1	.169	.171	5.46
1.0	.061	.071	.073
5	.028	.030	.043
10	.023	.022	.050

APPENDIX II

RADIATION DOSAGES AND DOSE RATES

1.0 ALLOWABLE DOSAGES

The following scale of allowable radiation dosages was established by the National Committee on Radiation Protection and by other similar bodies.

Maximum Allowable Dosages (Ref. 5)

Per Week	.3 rem
Per Quarter	3 rem
Per Year	5 rem
Per Lifetime	200 rem
Emergency Dose	25 rem*
Military Emergency Dose	200 rem

*Another 25 rem is allowable for emergencies in space.

2.0 TYPICAL DOSE RATES FROM THE VARIOUS SPACE ENVIRONMENTS

Environment	Dose Rate	Ref.
Normal Sea Level	.001 rem/day	73
Cosmic Rays (No Shielding)	.65 rem/week	3
Cosmic Rays (No Shielding)	5 rem/year	29
Cosmic Rays (No Shielding)	5 - 12 rem/year	73
Inner Van Allen Belt	6 rem/hr	73
Inner Van Allen Belt	20 rem/hr	73
Outer Van Allen Belt	200 rem/hr	73
Outer Van Allen Belt, Surface Dose	10^4 rad/hr	4
Aurora, Proton Surface Dose	500 rad/hr	21
Aurora-Electron Surface Dose	10^8 rad/hr	21
Solar Flare, Peak Levels	10 - 100 rem/hr	73
Solar Wind, Surface Dose	10^6 rad/hr	21

APPENDIX III

CALCULATIONS

1.0 ENERGY FLUX OF AURORAL ELECTRONS

Peak auroral flux (Ref. 21)	$= 10^{11} \text{ cm}^{-2} \text{ sec}^{-1}$
Peak electron energy (Ref. 21)	$= 50 \text{ Kev}$
Energy flux	$= 10^{11} \times 5 \times 10^4 \times 1.6 \times 10^{-12}$ $\times 10^{-7} (\text{cm}^{-2} \text{ sec}^{-1}) \times \text{ev} \times$ $(\text{erg ev}^{-1}) \times (\text{Joule erg}^{-1})$ $= 8 \times 10^{-4} \text{ watt cm}^{-2}$

2.0 ENERGY FLUX OF SOLAR WIND

Solar wind proton density (Ref. 42)	$= 10 \text{ cm}^{-3}$
Average proton velocity (Ref. 41)	$= 350 \text{ km sec}^{-1}$
Solar wind flux	$= 10 \times 350 \times 10^5$ $\text{cm}^{-3} \times \text{km sec}^{-1} \times \text{cm km}^{-1}$ $= 3.5 \times 10^8 \text{ cm}^{-2} \text{ sec}^{-1}$
Average proton energy (Ref. 21)	$= 1 \text{ Kev}$
Energy flux	$= 3.5 \times 10^8 \times 10^3 \times 1.6 \times 10^{-12}$ $\times 10^{-7} \text{ cm}^{-2} \text{ sec}^{-1} \times \text{ev}$ $\times (\text{erg ev}^{-1}) (\text{Joule erg}^{-1})$ $= 5.6 \times 10^{-7} \text{ watt cm}^{-2}$

3.0 ENERGY FLUX OF PLASMA CLOUD

Plasma cloud density (Ref. 65)	$= 10^3 \text{ protons cm}^{-3}$
Average proton velocity (Ref. 21)	$= 1500 \text{ km sec}^{-1}$
Plasma cloud flux	$= 10^3 \times 1500 \times 10^5 \text{ cm}^{-2} \text{ sec}^{-1}$ $= 1.5 \times 10^{11} \text{ cm}^{-2} \text{ sec}^{-1}$
Average proton energy (Ref. 66)	$= 5 \text{ Kev}$

Energy flux	$= 1.5 \times 10^{11} \times 5 \times 10^3 \times 1.6$ $\times 10^{-12} \times 10^{-7} \text{ cm}^{-2} \text{ sec}^{-1}$ $\times \text{kev} \times (\text{ev kev}^{-1}) (\text{erg ev}^{-1})$ (Joule erg^{-1}) $= 1.2 \times 10^{-4} \text{ watt cm}^{-2}$
-------------	---

4.0 ENERGY FLUX OF SOLAR PROTON BEAM

Typical proton flux (Ref. 21)	$= 10^4 \text{ cm}^{-2} \text{ sec}^{-1}$
Average proton energy (Estimated)	$= 20 \text{ Mev}$
Energy flux	$= 10^4 \times 20 \times 10^6 \times 1.6 \times 10^{-12}$ $\times 10^{-7}$ $= 3.2 \times 10^{-8} \text{ watt cm}^{-2}$

5.0 TYPICAL 1-Bev PROTON FLUX FROM ACCELERATOR

No. of protons pulse ⁻¹	$= 10^{11} \text{ pulse}^{-1}$
No. of pulses min ⁻¹	$= 100$
Area to be irradiated	$= 6600 \text{ ft}^2$ $= 6.13 \times 10^5 \text{ cm}^2$
No. of protons/sec	$= 10^{11} \times 100 \times 1/60$ $(\text{pulse}^{-1} \times \text{pulses min}^{-1})$ $\text{min sec}^{-1})$ $= 1.67 \times 10^{11} \text{ sec}^{-1}$
Proton flux	$= 1.67 \times 10^{11} \div 6.13 \times 10^5$ $= 2.72 \times 10^5 \text{ cm}^{-2} \text{ sec}^{-1}$

APPENDIX IV

HIGH ENERGY PARTICLE ACCELERATORS

1.0 TYPES OF ACCELERATORS

Particle accelerators can be divided into four main classes:

- a. resonance accelerators
- b. high voltage electrostatic devices
- c. betatrons and
- d. linear accelerators

2.0 RESONANCE ACCELERATORS

The principle of operation (Ref. 75) of the resonance accelerator is based upon the injection of a moving, charged particle into a time-varying electric and/or magnetic field. By properly selecting the frequency of the varying field(s), the particle can acquire energy continuously from the field(s).

2.1 Cyclotron

The earliest type of such an accelerator is the cyclotron (Ref. 75). The cyclotron consists, basically, of two "D"-shaped magnets, back to back. A high frequency electric field is applied across the small gap between the "D" uprights.

The charged particle is injected from an ion source at the center of the machine and is accelerated across the gap by the electric field. Upon entry into the "D" portion, the particle is acted upon by the magnetic field. This latter field causes the particle to turn gradually through 180 deg and re-enter the gap. Given the proper injection and frequency conditions, the particle would reach the gap at the time the electric field had reached the peak point of the reversed field polarity. The particle would therefore be accelerated across the gap and would enter the second "D" section with greater energy. The magnetic field again turns the particle through 180 deg, but the radius of curvature of the path is larger because of the greater particle energy. Viewed from above, the trajectory resembles a spiral.

The frequency of particle rotation, called the cyclotron frequency, is given by:

$$\begin{aligned}\omega &= \frac{Hce}{T} \\ &= Hce \frac{\sqrt{1 - (V/c)^2}}{1/2 M_0 V^2}\end{aligned}$$

where:

- ω = cyclotron frequency
- H = magnetic field intensity
- e = electric charge
- T = kinetic energy
- M_0 = rest mass
- c = velocity of light
- v = velocity of the particle

As the particle energy (and hence velocity) increases, the cyclotron frequency decreases because of the increase in velocity and also because of the relativistic mass increase experienced by the particles. The decrease in cyclotron frequency gradually causes the particle to drop out of synchronism with the varying electric field. The energy gain thus decreases continuously until, at some point, the particle arrives at the gap when the field is repulsive. It therefore loses energy and slows down slightly. Thus, a maximum energy is reached on the order of 10 to 25 Mev for protons.

Cyclotrons are unable to accelerate electrons to high energies since electrons reach close to the velocity of light (and hence the relativistic mass effect comes into play) at energies of a few Mev.

2.2 Synchrocyclotron

To overcome the relatively low energy maximum of the cyclotron, the synchrocyclotron (Ref. 77) using variable frequency electric and/or magnetic field was developed in the 1940's.

In the frequency-modulated cyclotron, the frequency of the applied radio-frequency field is lowered in step with the decreasing cyclotron frequency of the charged particles. Energies of hundreds of Mev are possible. A typical (Ref. 79) machine of this type is the C. E. R. N. (Council for European Nuclear Research) machine at Geneva, which produces protons at 600 Mev.

A second type of synchrotron is the electron synchrotron (sometimes called the betatron - synchrotron). In this machine, the electrons are accelerated by the betatron process (see later) up to several Mev. Basically, this is done by increasing the magnetic field intensity to compensate for the relativistic mass increase. As the magnets reach saturation, a high frequency electric field is applied. Since the electrons have been travelling at close to the speed of light from quite low energies, further energy increase comes from mass accretion. Since the velocity is essentially constant, the radius of the orbit varies only slightly, simplifying the magnet design. Lowering of the frequency of the electric field permits very high energies to be reached.

A third variant of the synchrotron is the proton synchrotron. In this machine, the electric and magnetic fields are varied in unison to maintain a constant orbital radius during acceleration in the non-relativistic range. Once relativistic effects become noticeable, the electric field frequency is fixed while the magnetic field intensity continues to increase. Examples of such machines are the cosmotron at Brookhaven National Laboratory, producing 3-Bev protons, the Bevatron at the University of California, producing 6.2-Bev protons, and a 10-Bev proton producer (Ref. 79) at the Joint Institute for Nuclear Research in Dubna, near Moscow. A few statistics on the Russian machine are enough to highlight the problem areas of this class of accelerator. The electromagnet for the accelerator is 56 meters (approximately 200 feet) in diameter and weighs about 36,000 tons. It has an overall power consumption of 150 mw.

The basic limitation of the synchrotron class of accelerators is that, to maintain particle stability in the orbit (and so reduce the loss of particles from the machine), the magnetic field strength must be reduced towards the outside of the orbital path. This feature means that, as the particle approaches the edge, the decrease in the magnetic field strength causes the cyclotron frequency to decrease further.

The second limitation is that, whenever a strong magnetic field accelerates an electron radially, the electron emits photon radiation (Ref. 80) in a broad spectrum (synchrotron radiation). In addition, during the emission process, the electron momentum must change in discrete amounts, thereby initiating oscillations in the orbit that grow with increasing electron energy and time.

2.3 Alternating Gradient

The most advanced types of resonance accelerators make use of the alternating gradient or strong focusing principle (Refs. 78, 79, and 80). In this method (see Fig. 9) the configuration of the magnetic field is varied

regularly around the orbital path. The positive gradient magnets have a gap height that decreases as the radius increases (Fig. 10a). The increased field intensity acts to repel the particles towards the center (Fig. 10b). The negative gradient magnets possess flux lines that curve outwards. As a result, particles below the center plane experience a force acting upwards while those above the plane experience a force that pushes them down. While each magnet acts to reduce the focussing effect of its immediate neighbor, the overall closed circuit effect is strong, focussing both radially and vertically; and orbital stability is improved by an order of magnitude. Accelerators using this principle are in operation at Geneva and Brookhaven at 28-Bev and 32-Bev levels, respectively, for protons.

A further improvement on this method is found in the Fixed Field Alternating Gradient (FFAG) machines. The principle here is to accelerate many bunches of particles in sequence to an intermediate energy and to accumulate them (or beam stack them) in an alternating gradient - stabilized orbit. The entire stacked beam is then carried to a much higher energy by a conventional synchrotron operation. Much higher beam intensities result.

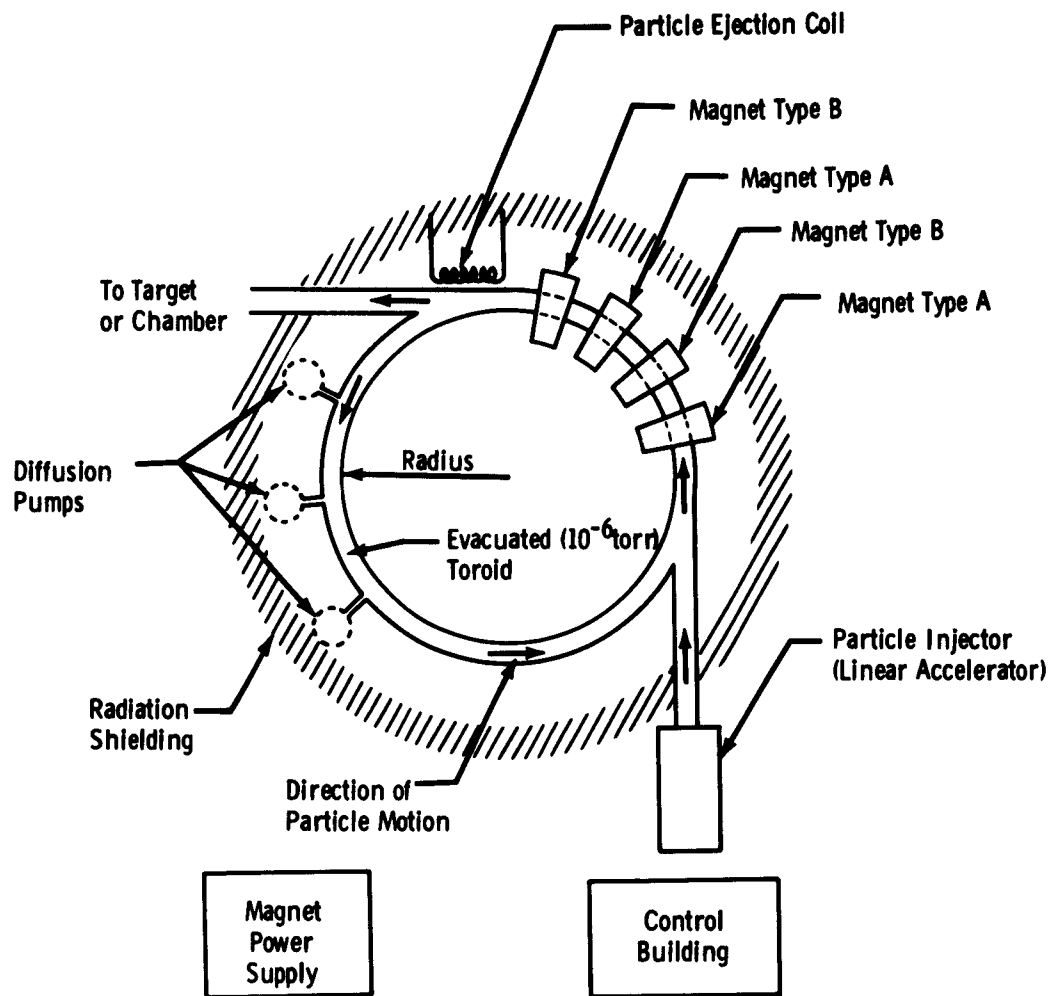
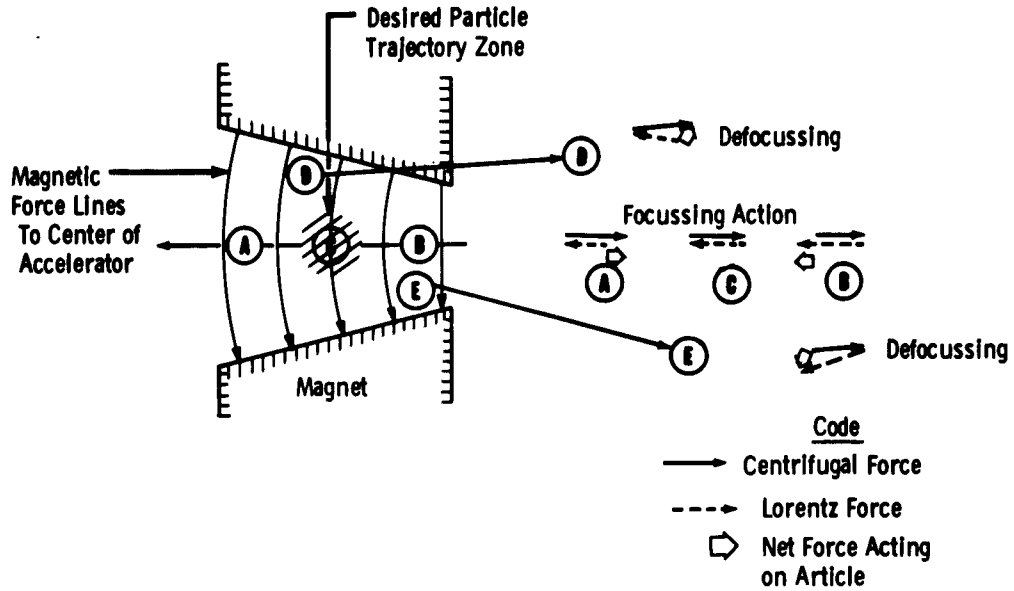
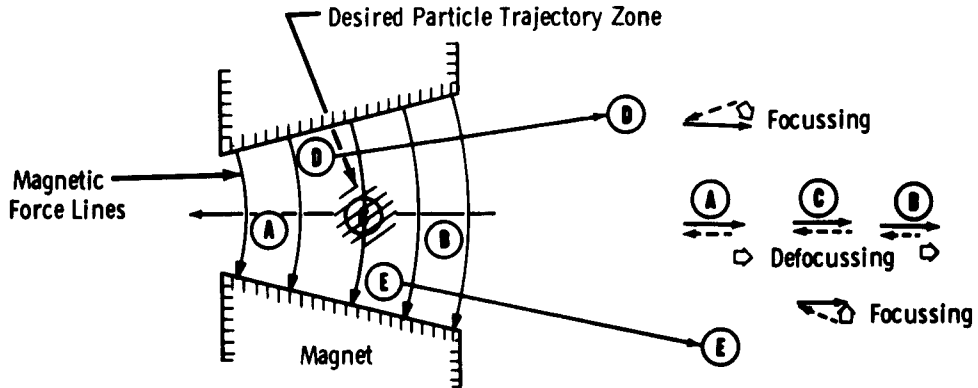


Fig. 9 Typical Alternating Gradient Accelerator



a. Magnet Type A (Restoring Force Stabilizes Orbit in Horizontal Plane but Defocusses Beam in Vertical Plane.)



b. Magnet Type B (Restoring Force Stabilizes Orbit in Vertical Plane but Defocusses Beam in Horizontal Plane.)

Fig. 10 Alternating Gradient Principle

3.0 HIGH VOLTAGE ELECTRO-STATIC ACCELERATORS

The most common high voltage accelerator is the Van de Graaff generator (Refs. 81 and 82). In this machine, a high voltage generator is used to place charges of the desired sign on a moving belt of rubber, silk, or other suitable material. The belt conveys the charge to a hollow sphere, where a rake removes it and deposits it on the sphere surface. As a result, the potential of the sphere can rise as high as 8 to 10 Mev. Proton beam currents of several micro-amperes are readily available. These currents contain almost mono-energetic particles. The Van de Graaff is easy to operate, and the output voltage is readily controlled.

4.0 THE BETATRON

The betatron is a device to produce high energy electrons. An alternating magnetic field is produced parallel to the axis of the evacuated toroidal chamber within which the electrons travel. This field produces an electromotive force that accelerates the electrons in their orbit, thereby increasing their energy. The field also produces a radial force that keeps the electrons moving in a circular path. As the electron energy increases, the magnetic field strength must increase. At the same time, the electron radiates increasing amounts of electromagnetic energy, and perturbing oscillations are generated as described previously. Energies up to approximately 300 Mev have been obtained, but extraction of the electron pulse is difficult to accomplish. Normally, if X-rays are required, a target is placed inside the toroid.

5.0 LINEAR ACCELERATORS

The final type of accelerator to be surveyed is the linear accelerator or linac. It comes in two design varieties. The first type accelerates charged particles electrostatically by passing them through successive sets of drift tubes, each drift tube being longer than the preceding one to compensate for the increasing velocity of the particle. In the second variety, the charged particles "ride" (Ref. 83) an electromagnetic wave. This guiding wave, usually produced by a klystron or magnetron, is generated with a mode in which the electric field vector is parallel to the axis of the linac tube.

The linear accelerator can be designed to give energies from a few Mev to 1 Bev. They are "relatively" simple to build and operate, but aligning the tube is critical. In many installations, an X-ray target is inserted into the tube, and the resulting, compact, X-ray generator finds wide use in industrial radiography.

6.0 ACCELERATOR PROBLEM AREAS

To accelerate protons and heavy ions, machines using the resonance principle must be used; however, the increasing complexity of these machines as the particle energy increases is vividly illustrated in Table 4.

Table 4 shows that increasing energy goes hand-in-hand with increased cost and complexity, the latter being evidenced in the physical size of the magnet. Careful detailed design of the foundation is required, for the settling must be uniform. For example, the magnet for the Cambridge electron accelerator (Ref. 80) is supported on heavy girders, which in turn rest on jacks and a traverse mechanism. This structure is supported on pilings that are mechanically isolated from the building. This complexity is required for the alignment of the magnet. In addition, inhomogenities in the magnetic field must be corrected or removed, lest an excessive proportion of the particle burst be lost through escape from the orbital track. For the same reason, the torodial track must be evacuated to at least 10^{-6} torr.

TABLE 4
CHARACTERISTICS OF TYPICAL ACCELERATORS

Machine Type	Ref.	Cost $\times 10^6$	Proton Energy	Magnet Weight, tons	Normal Power Load	Orbital Radius, M	No. of Particles Pulse^{-1}	Pulses min^{-1}
Cyclotron	84	?	9 Mev	41	30 kw	.35	4×10^{10}	Cont.
Cyclotron	85	\$5*	8 Mev	180	86 kw	.84	12.5×10^{13}	Cont.
F. M. Cyclotron	78	?	600 Mev	2500	?	2.27	10^{11}	3300
Cosmotron	86	\$7	3 Bev	2000	?	9.15	10^9	12
Bevatron	79	?	6.2 Bev	10^4	?	15	10^{11}	10
Electron Synchrotron	80	?	6 Bev (Electron)	288	1 mw	36	10^{11}	3600
Proton Synchrotron	85	?	10 Bev	36×10^3	10 mw	28	10^9	5
Zero Grad Synchrotron	87 89	\$29 \$47	12.5 Bev	?	117 mw	30.5	?	?
Alternating Gradient Synchrotron	89	\$31	32 Bev	4×10^3	?	20	2×10^{11}	2

*Estimated

To reduce the secondary radiation hazard, the whole accelerator requires protective shielding. For example, the Cambridge accelerator

(Ref. 80) is located ten feet below the ground, while the C. E. R. N. Synchrotron has a barium concrete wall six meters thick around it. The operations building is protected by another wall, this time of earth.

Yet another problem is that of extracting and focusing the high energy beams. One method used is to pulse an auxiliary electromagnet and so perturb the particle orbit.

Finally, the particle streams are highly collimated and very discrete in energy. It is not known if it would be possible to diverge the beam in such a manner as to irradiate uniformly an area measured in thousands of square feet. It will also be difficult to match the energy spectrum. Possibly, the spectrum should be divided into distinct ranges. A number of accelerators would then be used to match the desired fluxes in each energy range, either simultaneously or, more likely, in succession.

REFERENCES

1. Scarsi, L. "Cosmic Radiation." American Journal of Physics, Vol. 28, No. 3, March 1960, p. 213.
2. Lehr, S. N., and Tronolone, V. J. "The Space Environment and Its Effects on Materials and Component Parts." IRE Transactions on Reliability and Quality Control, ROC-10, No. 2, August 1961, p. 24.
3. Wallner, L. E., and Kaufman, H. R. "Radiation Shielding for Manned Space Flight." NASA Technical Note D-681, July 1961.
4. Langham, W. H. "Some Radiation Problems of Space Conquest." Astronautik, Space Medicine Symposium, Vol. 2, No. 4, 1961, p. 213.
5. Jacobs, G. J. (editor). "Proceedings of Conference on Radiation Problems in Manned Space Flight." NASA Technical Note D-588, June 21, 1960.
6. Sandeman, T. F. "The Proton Peril." Spaceflight, Vol. 4, No. 4, July 1962, p. 115.
7. Jaffe, L. D. and Rittenhouse, J. B. "Behavior of Materials in Space Environments." American Rocket Society Journal, Vol. 32, No. 3, March 1962, p. 320.
8. Barnes, R. S. "The Effect of the Radiations Encountered by Materials in Space." Journal of British Interplanetary Society, Vol. 18, No. 9, May - June 1962, p. 377.

9. Brinkman, J. A. "Production of Atomic Displacements by High Energy Particles." American Journal of Physics, Vol. 24, No. 4, April 1956, p. 246.
10. Harwood, J. J., et. al. The Effects of Radiation on Materials. Reinold Publishing Co., New York, 1958.
11. Seitz, F. "Radiation Effects in Solids." Physics Today, Vol. 5 and 6, June 1952, p. 6.
12. Moore, W. J. "The Ionic Bombardment of Solid Surfaces." The American Scientist, Vol. 48, No. 2, June 1960, p. 109.
13. Redus, J. R. "Sputtering of a Vehicle's Surface in a Space Environment." NASA Technical Note D-1113, June 1962.
14. Hollaender, A., and Stapleton, G. E. "Ionizing Radiation and the Living Cell." Scientific American, Vol. 201, No. 3, September 1959, p. 94.
15. Artandi, C. "Plastics Dosimetry." Nucleonics, Vol. 17, No. 10, October 1956, p. 62.
16. Smits, F. M., Smith, K. D., and Brown, W. L. "Solar Cells for Communications Satellites in the Van Allen Belts." Journal of the British Institute of Radio Engineers, Vol. 22, No. 2, August 1961, p. 161.
17. Hulten, W. D., Honaker, W. C., and Patterson, J. L. "Irradiation Effects of 22 and 240 Mev Protons on Several Transistors and Solar Cells." NASA Technical Note D-718, April 1961.
18. Innes, R. "Radiation and Other Environmental Effects on Satellites." Journal of the British Institute of Radio Engineers, Vol. 22, No. 3, September 1961, p. 241.
19. Al'Pert, Ya L. "Investigation of the Ionosphere and of the Interplanetary Gas with the Aid of Artificial Satellites and Space Rockets." Soviet Physics - Uspekhi, Vol. 3, No. 4, January - February 1961, p. 479.
20. Hanson, W. B. "Structure of the Ionosphere." Satellite Environment Handbook, Ed. by Johnson, F. S., Stanford University Press, 1961, p. 27.
21. Lee, J. C. "Penetrating Radiation." Space Materials Handbook, Ed. by Goetzl, C. G., and Singletary, J. B., Lockheed Missiles and Space Company (AF 04(647) - 673), p. 51.
22. Handbook of Geophysics (Revised Edition). United States Air Force, Geophysics Research Directorate, AFCRC, ARDC, The MacMillan Company, New York, 1961.

23. Krasovskii, V. I. "Some Problems of Auroral Physics." American Rocket Society Journal, Vol. 30, No. 11, November 1960, p. 1065.
24. Dessler, A. J., Hanson, W. B., and Parker, E. N. "Formation of the Geomagnetic Storm Main Phase Ring Current." Journal of Geophysical Research, Vol. 66, No. 1, November 1961, p. 3631.
25. Hart, E. M. "Effects of Outer Space Environment Important to Simulation of Space Vehicles." ASD Technical Report 61-201, August 1961.
26. Freden, S. C., and White, R. S. "Particle Fluxes in the Inner Radiation Belt." Journal of Geophysical Research, Vol. 65, No. 5, May 1960, p. 1377.
27. Hess, W. H. "The Radiation Belt Produced by Neutrons Leaking Out of the Atmosphere of the Earth." Journal of Geophysical Research, Vol. 65, No. 10, October 1960, p. 3107.
28. Kellog, P. J. "Electrons of the Van Allen Region." Journal of Geophysical Research, Vol. 65, No. 9, September 1960, p. 2705.
29. Masley, A. J., and Goedeke, A. D. "Space Radiation - Its Nature and Properties." Aerospace Engineering, Vol. 21, No. 6, June 1962, p. 21.
30. Rothwell, P., and Mc Ilwain, C. E. "Magnetic Storms and the Van Allen Radiation Belts." Journal of Geophysical Research, Vol. 65, No. 3, March 1960, p. 799.
31. Dessler, A. J. and Karplus, R. "Some Properties of the Van Allen Radiation." Physical Review Letters, Vol. 4, No. 6, March 15, 1960, p. 271.
32. Fan, C. Y., Meyer, P., and Simpson, J. A. "Dynamics and Structure of the Outer Radiation Belt." Journal of Geophysical Research, Vol. 66, No. 9, September 1961, p. 2607.
33. Rothrock, A. M. "The Costs of Space Operation." Spaceflight, Vol. 4, No. 4, July 1962, p. 113.
34. Crawford, J. A. "Fermi Acceleration of Electrons in Outer Van Allen Belt." Physical Review Letters, Vol. 3, No. 7, October 1, 1959, p. 316.
35. Gold, T. "Cosmic Rays and the Interplanetary Medium." Astronautics, Vol. 7, No. 8, August 1962, p. 43.

36. Lockwood, J. A. "Decrease of Cosmic Ray Intensity." Journal of Geophysical Research, Vol. 65, No. 1, January 1960, p. 27.
37. Athay, R. G., and Warwick, C. S. "Indices of Solar Activity." Advances in Geophysics, Vol. 8, Ed. by Landsberg, H. E., and Van Meghem, Jr., Academic Press, 1961, p. 1.
38. Friedman, H. "Solar Radiation." Astronautics, Vol. 7, No. 8, August 1962, p. 14.
39. Parker, E. "Extension of the Solar Corona Into Interplanetary Space." Journal of Geophysical Research, Vol. 64, No. 11, November 1959, p. 1675.
40. Warwick, J. W. "Some Remarks on the Interaction of Solar Plasma and The Geomagnetic Field." Journal of Geophysical Research, Vol. 64, No. 4, April 1959, p. 389.
41. Kolcum, E. H. "First Venus Data Still Assured." Aviation Week, Vol. 77, No. 16, October 15, 1962, p. 30.
42. White, M. L., and Wyller, A. A. "Interplanetary Gas and Magnetic Fields." Space and Planetary Environments, Ed. by Shea Valley, AFCRL -62-270, January 1962, p. 1.
43. Ogilvie, K. W. "Solar Protons." NASA Technical Note D-1139, July 1962.
44. Fireman, E. L. "Density of the Solar Flare Plasma." Journal of Geophysical Research, Vol. 67, No. 13, November 1962, p. 4890.
45. Axford, W. I. "The Interaction Between the Solar Wind and the Earth's Magnetosphere." Journal of Geophysical Research, Vol. 67, No. 10, September 1962, p. 3791.
46. Ortner, J., Hultqvist, B., et. al. "Cosmic Noise Absorption Accompanying Geomagnetic Storm Sudden Commencements." Journal of Geophysical Research, Vol. 67, No. 11, October 1962, p. 4169.
47. Peters, B. "Progress in Cosmic Ray Research Since 1947." Journal of Geophysical Research, Vol. 64, No. 2, February 1959, p. 155.
48. Warwick, J. W. "The Source of Solar Flares." Publication of the Astronomical Society of the Pacific, Vol. 74, No. 439, August 1962, p. 302.
49. Anderson, K. W. "Preliminary Study of Prediction Aspects of Solar Cosmic Ray Events." NASA Technical Note D-700, April 1961.
50. Fichtel, C. E., Kniffen, D. A., and Ogilvie, K. W. "Sept 26, 1960 Solar Cosmic Ray Event." Journal of Geophysical Research, Vol. 67, No. 10, September 1962, p. 3669.

51. Waddington, C. J. "Hazard of Corpuscular Solar Radiation to Manned Space Flight." Journal of the British Interplanetary Society, Vol. 18, No. 7, January - February 1962, p. 277.
52. Hill, G. E. "Effects of Corpuscular Emissions on Polar Ionosphere Following Solar Flares." Journal of Geophysical Research, Vol. 66, No. 8, August 1961, p. 2329.
53. Dodson, H. W., and Hedeman, E. R. "Solar Flares Observed During I. G. Y." Journal of Geophysical Research, Vol. 65, No. 1, January 1960, p. 123.
54. Ney, E. P., and Stein, W. A. "Solar Protons, Alpha Particles and Heavy Nuclei in November 1960." Journal of Geophysical Research, Vol. 67, No. 6, June 1962, p. 2087.
55. Obayashi, T., and Hakura, Y. "Solar Corpuscular Radiation and Polar Ionospheric Disturbances." Journal of Geophysical Research, Vol. 65, No. 10, October 1960, p. 3131.
56. Gold, T. "Plasma and Magnetic Fields in the Solar System." Journal of Geophysical Research, Vol. 64, No. 11, November 1959, p. 1665.
57. Beard, D. B., and Johnson, F. S. "Ionospheric Limitations on Attainable Satellite Potential." Journal of Geophysical Research, Vol. 66, No. 12, December 1961, p. 4113.
58. Jastrow, R. "Artificial Satellites and the Earth's Atmosphere." Scientific American, Vol. 201, No. 2, August 1959, p. 37.
59. Kraus, J. D., Higgy, R. C., and Crone, W. R. "The Satellite Ionization Problem." Proceedings of the IRE, Vol. 48, No. 4, April 1960, p. 672.
60. Kraus, J. D. and Tiuri, M. E. "Observations of Satellite - Related Ionization Effects Between 1958 and 1960." Proceedings of the IRE, Vol. 50, No. 10, October 1962, p. 2076.
61. Gaumer, R. E. and McKellar, L. A. "Thermal Radiative Control Surfaces for Spacecraft." Lockheed Missiles and Space Division, LMSD - 704014, March 1961.
62. Vosteen, L. F. (Editor). "Environmental Problems of Space Flight Structures." NASA Technical Note D-1474, October 1962.
63. Liszka, L. "Drop-Out Phenomenon Observed in Satellite 1958 δ_2 Transmissions." Journal of Geophysical Research, Vol. 66, No. 5, May 1961, p. 1573.
64. Foelsche, T. "Current Estimates of Radiation Dosages in Space." NASA Technical Note D-1267, July 1962.

65. Reiffel, L. "Structural Damage and Other Effects of Solar Plasma." American Rocket Society Journal, Vol. 30, No. 30, March 1960, p. 258.
66. Reiffel, L. "Structural Effects and Particle Content of Interplanetary Space." American Rocket Society Journal, Vol. 30, No. 7, July 1960, p. 654.
67. Anderson, K. A., and Fichtel, C. E. "Discussions of Solar Proton Events and Manned Space Flight." NASA Technical Note D-671, March 1961.
68. Johnson, F. S. "Physics of the Atmosphere and Space." Astronautics, Vol. 7, No. 11, November 1962, p. 72.
69. Levy, R. H. "Radiation Shielding of Space Vehicles by Means of Superconducting Coils." American Rocket Society Journal, Vol. 31, No. 11, November 1961, p. 1568.
70. Kash, S. W., and Tooper, R. F. "Active Shielding for Manned Space Craft." Astronautics, Vol. 7, No. 9, September 1962, p. 68.
71. Anon. "Nuclear Space News - New Space Lab Will Simulate Space Radiation." Nucleonics, Vol. 20, No. 12, December 1962, p. 28.
72. Anon. "Tuning up a Linear Accelerator." Engineering, Vol. 194, No. 5030, September 14, 1962, p. 361.
73. Naugle, J. E. "Space Radiation Levels." Nucleonics, Vol. 19, No. 4, April 1961, p. 89.
74. Fano, V. "Gamma Ray Attenuation - Basic Processes." Nucleonics, Vol. 11, No. 8, August 1963, p. 10.
75. De Groot, W. "Cyclotron and Synchocyclotron." Philips Technical Review, Vol. 12, No. 3, September 1950, p. 65.
76. Livingston, M. S. "Early Development of Particle Accelerators." American Journal of Physics, Vol. 27, No. 9, December 1959, p. 626.
77. Blumenthal, I. S. "The Operating Principles of Synchrotron Accelerators." American Journal of Physics, Vol. 21, No. 3, March 1953, p. 164.
78. Gentner, W. "C. E. R. N. - 600 Mev Synchocyclotron at Geneva, Part I, Object and Design." Phillips Technical Review, Vol. 22, No. 5, March 6, 1961, p. 141.
79. Veksler, V. I. "The Present State of the Problem of Acceleration of Atomic Particles." Soviet Physics - Uspekhi, Vol. 3, No. 1, September - October 1958, p. 54.

65. Reiffel, L. "Structural Damage and Other Effects of Solar Plasma." American Rocket Society Journal, Vol. 30, No. 30, March 1960, p. 258.
66. Reiffel, L. "Structural Effects and Particle Content of Interplanetary Space." American Rocket Society Journal, Vol. 30, No. 7, July 1960, p. 654.
67. Anderson, K. A., and Fichtel, C. E. "Discussions of Solar Proton Events and Manned Space Flight." NASA Technical Note D-671, March 1961.
68. Johnson, F. S. "Physics of the Atmosphere and Space." Astronautics, Vol. 7, No. 11, November 1962, p. 72.
69. Levy, R. H. "Radiation Shielding of Space Vehicles by Means of Superconducting Coils." American Rocket Society Journal, Vol. 31, No. 11, November 1961, p. 1568.
70. Kash, S. W., and Tooper, R. F. "Active Shielding for Manned Space Craft." Astronautics, Vol. 7, No. 9, September 1962, p. 68.
71. Anon. "Nuclear Space News - New Space Lab Will Simulate Space Radiation." Nucleonics, Vol. 20, No. 12, December 1962, p. 28.
72. Anon. "Tuning up a Linear Accelerator." Engineering, Vol. 194, No. 5030, September 14, 1962, p. 361.
73. Naugle, J. E. "Space Radiation Levels." Nucleonics, Vol. 19, No. 4, April 1961, p. 89.
74. Fano, V. "Gamma Ray Attenuation - Basic Processes." Nucleonics, Vol. 11, No. 8, August 1963, p. 10.
75. De Groot, W. "Cyclotron and Synchocyclotron." Philips Technical Review, Vol. 12, No. 3, September 1950, p. 65.
76. Livingston, M. S. "Early Development of Particle Accelerators." American Journal of Physics, Vol. 27, No. 9, December 1959, p. 626.
77. Blumenthal, I. S. "The Operating Principles of Synchrotron Accelerators." American Journal of Physics, Vol. 21, No. 3, March 1953, p. 164.
78. Gentner, W. "C. E. R. N. - 600 Mev Synchocyclotron at Geneva, Part I, Object and Design." Phillips Technical Review, Vol. 22, No. 5, March 6, 1961, p. 141.
79. Veksler, V. I. "The Present State of the Problem of Acceleration of Atomic Particles." Soviet Physics - Uspekhi, Vol. 3, No. 1, September - October 1958, p. 54.

80. Livingston, M.S., and Shurcliff, W. A. "The Cambridge Electron Accelerator." Science, Vol. 134, No. 3486, October 20, 1961, p. 1186.
81. Ruck, R. D. Introduction to Atomic and Nuclear Physics. Appleton - Century - Crofts, Inc., New York, 1958.
82. Semat, H. "Introduction to Atomic and Nuclear Physics." Rinehart and Co., Inc., New York, April 1960.
83. Bareford, C. F. and Kelliker, M. G. "15 Mev Linear Accelerator." Phillips Technical Review, Vol. 15, No. 1, July 1953. p. 1.
84. Henderson, M. C. and White, M. G. "Design and Operation of a Large Cyclotron." Review of Scientific Instruments, Vol. 9, No. 1, January 1938, p. 19.
85. Halliday, D. Introductory Nuclear Physics, 2nd Edition, Wiley and Sons, New York, January 1962.
86. Veksler, V. I. "Start up of a 10 Bev Synchrophasotron." Proceedings of Second United Nations International Conference on the Peaceful Uses of Atomic Energy, Vol. 30, United Nations, Geneva, 1958.
87. Anon. "Digging Deeper into the Atom." Business Week, November 17, 1962, p. 140.
88. Anon. "Construction to Begin on 10-45 Bev Stanford Linac Complex." Nucleonics, Vol. 20, No. 1, January 1962, p. 23.
89. Beth, R. A., and Lasky, C. "The Brookhaven Alternating Gradient Synchrotron." Science, Vol. 128, No. 3336, December 5, 1958, p. 1393.

<p>Arnold Engineering Development Center Arnold Air Force Station, Tennessee Rpt. No. AEDC-TDR-63-118. THE SIMULATION OF HIGH ENERGY PENETRATING RADIATIONS. July 1963, 69 p. incl 89 refs., illus., tables. Unclassified Report</p> <p>The basis of this study has been a search of current literature to determine the penetrating radiation characteristics of the space environments and to assess the necessity for reproducing such environments completely or in part. This study of the radiation environments led to the formulation of some possible test objectives. The advantages and disadvantages of performing these objectives in the proposed chamber are listed. Two main simulation approaches, one using radiation from isotopic sources and the other using particles generated by high energy accelerators, are feasible, but only the latter is worthy of consideration, taking into account the size of the vehicles to be tested. Furthermore, only the second method can provide a worthwhile match of the energy and flux spectra of space radiation.</p>	<ol style="list-style-type: none">1. Space environmental conditions2. Cosmic rays3. Nuclear particles4. Radiation effects5. Simulation6. Electromagnetic waves7. Shielding8. Bibliographies <ol style="list-style-type: none">I. AFSC Program Area N/AII. Contract AF 40(600)-1000III. ARO, Inc., Arnold AF Sta, Tenn.IV. Sqd Ldr G. MacFarlaneV. Available from OTSVI. In ASTIA Collection	<p>Arnold Engineering Development Center Arnold Air Force Station, Tennessee Rpt. No. AEDC-TDR-63-118. THE SIMULATION OF HIGH ENERGY PENETRATING RADIATIONS. July 1963, 69 p. incl 89 refs., illus., tables. Unclassified Report</p> <p>The basis of this study has been a search of current literature to determine the penetrating radiation characteristics of the space environments and to assess the necessity for reproducing such environments completely or in part. This study of the radiation environments led to the formulation of some possible test objectives. The advantages and disadvantages of performing these objectives in the proposed chamber are listed. Two main simulation approaches, one using radiation from isotopic sources and the other using particles generated by high energy accelerators, are feasible, but only the latter is worthy of consideration, taking into account the size of the vehicles to be tested. Furthermore, only the second method can provide a worthwhile match of the energy and flux spectra of space radiation.</p>	<ol style="list-style-type: none">1. Space environmental conditions2. Cosmic rays3. Nuclear particles4. Radiation effects5. Simulation6. Electromagnetic waves7. Shielding8. Bibliographies <ol style="list-style-type: none">I. AFSC Program Area N/AII. Contract AF 40(600)-1000III. ARO, Inc., Arnold AF Sta, Tenn.IV. Sqd Ldr G. MacFarlaneV. Available from OTSVI. In ASTIA Collection